

The University of Manitoba

THERMOGRAVIMETRIC ANALYSIS AND  
MASS SPECTRAL STUDIES OF SOME  
TRANSITION METAL VIC - DIOXIMATES

by

Daniel K. C. Fung

A Thesis

Submitted to

the Faculty of Graduate Studies and Research

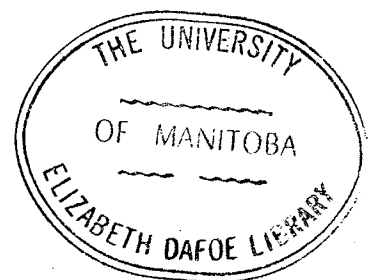
In Partial Fulfilment

of the Requirements for the Degree

MASTER OF SCIENCE

Winnipeg, Manitoba

December, 1969



## ACKNOWLEDGEMENT

I owe my deepest appreciation to my Supervisor, Dr. J. B. Westmore for his patience and careful guidance throughout the whole course of this work. I also have to thank Dr. C. Reichert and Mr. D. Lin for their help and suggestions.

Without the care and thoughtfulness of the Pollard's family my study and stay in Canada would have been less valuable and my gratitude to them cannot be expressed in words. Special thanks are also due to Miss Winnie Chan for the encouragement and for her help in the typing.

I am also grateful to all my friends and to the whole Chemistry Department for providing me with such immense opportunity and tremendous experience. I also would like to express my thanks to Miss D. Ostlere and Mr. T. Kiezer and Mr. L. Krucynski for helping me with the pictures and spectra.

To My Parents and Brother

## ABSTRACT

The Ni(II), Pd(II) and Pt(II) complexes of dimethylglyoxime, diphenylglyoxime,  $\alpha$ -furildioxime, nioxime and 4-methylnioxime have been studied by thermoanalytical and mass spectrometric means.

It is found that the decompositions of the vic-dioximates are affected by the presence of oxygen and that these decompositions are exothermic. All of the complexes are stable up to 250°C with the platinum complexes decomposing at the lowest temperatures, contrary to the general thermal stabilities of square planar complexes of this group of metals.

Mass spectra of the complexes were recorded with an electron energy of 50 volts and they show fair degrees of complexity, especially the nioxime and 4-methyl-nioxime complexes where decomposition of the cyclohexane ring also took place. General trends between the various metals and ligands are not clearly shown but participation through  $\pi$ -bonding of the metal  $p_z$  orbital in the stabilization of the ion is suggested. This participation might be expected to increase as the ease of oxidation of the metal increases, i. e.  $\text{Ni} < \text{Pd} \approx \text{Pt}$  so that the relative intensities of the  $(\text{P} - \text{OH})^+$  and  $(\text{P} - \text{R})^+$  ions should be in the sequence  $\text{Ni} > \text{Pd} \approx \text{Pt}$ . In fact, the opposite trend was found. This may be attributed to many factors among which atomic size of the metals and their relative ionization potentials might be important.

## TABLE OF CONTENTS

### CHAPTER ONE

General Survey of Literature Work -----	( 1 )
---	-------

### CHAPTER TWO

Thermogravimetric Analysis -----	( 9 )
Section I. Introduction -----	( 9 )
Section II. Instrumental - The Thermal Balance -----	( 10 )
Section III. Experimental - Sample Preparation and Instrument Calibration -----	( 16 )
(a) Sample Preparation -----	( 16 )
(b) Calibration of Instrument For Accurate Temperature Read-out -----	( 16 )
(c) TGA Mode Analysis -----	( 21 )
(d) DTG Mode Analysis -----	( 22 )
Section IV. Results and Discussions -----	( 22 )
(a) General -----	( 22 )
(b) Dimethylglyoximates -----	( 43 )
(c) Nioximates and 4-methyl-nioximates -	( 46 )
(d) Diphenylglyoximates and $\alpha$ -Furil- dioximates -----	( 46 )

### CHAPTER THREE

Mass Spectral Studies -----	( 49 )
-----------------------------	--------

Section I. Introduction -----	(49)
Section II. Instrumental - The Hitachi RMU - 6D Model -	(51)
Structure of Instrument -----	(51)
Types of Ions Formed under Electron Impact	(56)
Section III. Experimental - Mass Spectrometer Operation	
Conditions and Identification of Mass Spectra	(64)
Preparation of Samples -----	(64)
Operation Conditions -----	(64)
Identification of Mass Spectra -----	(65)
Section IV. Results and Discussions -----	(65)

#### CHAPTER FOUR

Summary and Conclusions -----	(89)
BIBLIOGRAPHY -----	(90)

## TABLE OF FIGURES

Fig.	1. Thermal Balance Components of Model TGS - 1 ----	( 11 )
	2. Schematic Diagram of Cahn RG Automatic Electrobalance -----	( 13 )
	3. Electrical and Gas Connections of Thermobalance Set-up -----	( 15 )
	4. Effect of Heat on Stirrup, Hangdown Wire and Sample Pan of Thermobalance in Air, Nitrogen and Vacuum -----	( 20 )
	5. Thermogram of Ni(DMG) <sub>2</sub> -----	( 25 )
	6. Thermogram of Pd(DMG) <sub>2</sub> -----	( 26 )
	7. Thermogram of Pt(DMG) <sub>2</sub> -----	( 27 )
	8. Thermogram of Ni(Niox) <sub>2</sub> -----	( 28 )
	9. Thermogram of Pd(Niox) <sub>2</sub> -----	( 29 )
	10. Thermogram of Pt(Niox) <sub>2</sub> -----	( 30 )
	11. Thermogram of Ni(4MNiox) <sub>2</sub> -----	( 31 )
	12. Thermogram of Pd(4MNiox) <sub>2</sub> -----	( 32 )
	13. Thermogram of Pt(4MNiox) <sub>2</sub> -----	( 33 )
	14. Thermogram of Ni(DPG) <sub>2</sub> -----	( 34 )
	15. Thermogram of Pd(DPG) <sub>2</sub> -----	( 35 )
	16. Thermogram of Pt(DPG) <sub>2</sub> -----	( 36 )
	17. Thermogram of Ni(α-DFD) <sub>2</sub> -----	( 37 )
	18. Thermogram of Pd(α-DFD) <sub>2</sub> -----	( 38 )
	19. Thermogram of Pt(α-DFD) <sub>2</sub> -----	( 39 )
	20. Thermograms of M(DPG) <sub>2</sub> Obtained in Vacuum ---	( 40 )
	21. Thermograms of M(α-DFD) <sub>2</sub> -----	( 41 )

Fig.	22.	Cross-sectional View of Ion Source of Hitachi RMU-6D Mass Spectrometer -----	( 54 )
	23.	Mass Dispersion in the Magnetic Field -----	( 55 )
	24.	Layout of Ion Source, Analyzer and Detector of RMU-6D Mass Spectrometer -----	( 57 )
		Mass Spectra of Vic-dioximates	
	25.	Dimethylglyoximates -----	( 67 )
	26.	Diphenylglyoximates -----	( 68 )
	27.	$\alpha$ -Furildioximates -----	( 69 )
	28.	Nioximates -----	( 70 )
	29.	4-methyl-nioximates -----	( 71 )
	30.	Comparison of Mass Spectrum of Ni(DMG) <sub>2</sub> -----	( 72 )
	31.	Schematic Diagram of Fragmentation Pattern of Vic - dioximates -----	( 80 )

## LIST OF TABLES

Table	I. Complexes Studied and Abbreviation used ----- (2)
	II. Bond Angles and Bond Lengths in the Metal Vic - dioximates and Related Compounds ----- (3)
	III. Molecular Weights and Colour of the Metal Vic - dioximates ----- (17)
	IV. Comparison of Apparent and Manufacturer's Values of Curie Points of Magnetic Standards - (19)
	V. Decomposition Temperatures of Vic - dioximates (23)
	VI. Residue Characteristics of Vic - dioximates after Heating in Air and in Nitrogen ----- (44)
	VII. IBM 360 Computer Program for Matching Peaks with Atoms ----- (66)
	VIII. Sample Temperature, Mass/charge Ratios for Metastable and Doubly - charged Ion Peaks for Dimethylglyoximates ----- (73)
	IX. Sample Temperature, Mass/charge Ratios for Metastable and Doubly - charged Ion Peaks for Diphenylglyoximates ----- (74)
	X. Sample Temperatures, Mass/charge Ratios for Metastable and Doubly - charged Ion Peaks for $\alpha$ - Furildioximates ----- (75)
	XI. Sample Temperature, Mass/charge Ratios for Metastable and Doubly - charged Ion Peaks for Nioximates ----- (76)
	XII. Sample Temperature, Mass/charge Ratios for Metastable and Doubly - charged Ion Peaks for 4 - methyl - nioximates ----- (77)
	XIII. Isotopic Ratio and Intensity Calculations of Some Species of Dimethylglyoximates ----- (87)

CHAPTER ONE  
GENERAL SURVEY  
OF  
LITERATURE WORK

Nickel, palladium and platinum vic-dioximates (1), especially those formed from dimethylglyoxime have been much studied by X-ray (2 - 8), infra-red (9), ultra-violet and visible (10, 11) spectroscopy. Their nucleation and generation (12, 13) and effects of pressure on them (14) have also been investigated. The tremendous amount of attention given to this group of inner-metallic complex salts (15) has been due to their low solubility and thus their use as gravimetric determination and / or separation reagents for nickel, palladium and platinum. (16, 17, 18) It is hoped that the study of the thermograms and mass spectra of some of these complexes will give a more thorough understanding of this particular group of compounds. We have made the study of the nickel, palladium and platinum complexes formed from the following dioximes (table I) :

1. Dimethylglyoxime
2. Diphenylglyoxime
3.  $\alpha$ -furildioxime
4. Nioxime
5. 4-Methyl-nioxime

It has been concluded (3) that most of these complexes have similar crystal structures. The metal-nitrogen (ligand) distances are characteristic of each metal, being similar to the metal-nitrogen (oxime) distances of other mono- or di- oxime complexes and shorter than the metal-nitrogen (amine) bond distances in the amine complexes. (See table II for comparison). The O-H-O bond distances are short

TABLE I. COMPLEXES STUDIED AND ABBREVIATION USED

M = Nickel, palladium and platinum (II)

OXIMES	FORMULA	STRUCTURE OF COMPLEX	ABBR. USED
$\begin{array}{c} R-C-C-R \\    \quad    \\ HO-N \quad N-OH \end{array}$			
Dimethylglyoxime	R = CH <sub>3</sub>		M(DMG) <sub>2</sub>
Diphenylglyoxime (benzildioxime)	R = Ph		M(DPG) <sub>2</sub>
$\alpha$ -furildioxime	R =		M( $\alpha$ -DFD) <sub>2</sub>
OXIMES			
Nioxime	R = H		M(Niox) <sub>2</sub>
4-Methyl-Nioxime	R = CH <sub>3</sub>		M(4MNiox) <sub>2</sub>

TABLE II. BOND LENGTHS AND BOND ANGLES IN THE METAL VIC-DIOXIMATES AND RELATED COMPOUNDS

SPECIFICATIONS AND ABBREVIATIONS:

Bond angles are in A

EMG = ethylmethylglyoxime

C - C = C - C bond distance between the dioxime groups

NiAO = Bis(2-amino-2-methyl-3-butanone-oximato) nickel(II) chloride monohydrate

Ni(SAD)<sub>2</sub> = salicylaldoxime-Ni(II)

a = J. R. Wiesner and E. C. Lingafelter, Inorg. Chem. 5, 1770 (1966)

b = R. Shintain, Acta Cryst, 13, 609 (1960)

c = Intramolecular Distances, 18, London Chem. Soc. 1965

HB = Handbook of Chemistry and Physics, 46th Edition

Compound	M-N distance	O-H-O distance	MNO bond angle	N-C distance	NCC bond angle	C-C	Ref.				
Ni(DMG) <sub>2</sub>	1.90	1.87	2.44	118	122	1.20	1.25	109	113	1.53	2, 7, 8
Pd(DMG) <sub>2</sub>	1.93	1.99	2.59-2.62	-	-	1.31	1.31	-	-	1.47	3, 8
Pt(DMG) <sub>2</sub>	1.93	1.95	3.03	134	135	1.27	1.38	117	113	1.57	2
Cu(DMG) <sub>2</sub>	1.93	1.96	2.53-2.70	121.5	125	1.22	1.27	114	110.5	1.53	3, 5, 8
NiAO	1.85	1.91	2.38	121.5	-	1.30	1.52	114	106	1.50	3
Ni(SAD) <sub>2</sub>	1.86	-	2.52	122	-	1.40	1.40	-	-	-	c
Ni(en) <sub>3</sub> (NO <sub>3</sub> ) <sub>2</sub>	2.12	-	-	-	-	1.50	1.50	111	-	1.50	a
Pd(en) <sub>2</sub> Cl <sub>2</sub>	2.04	2.03	-	-	-	1.47	1.48	107	-	1.51	a
Pt(SN) <sub>4</sub>	2.15	2.03	-	-	-	-	-	-	-	-	c
K <sub>4</sub> (Ni(NO <sub>2</sub> ) <sub>6</sub> )	2.15	-	-	-	-	-	-	-	-	-	c
K <sub>2</sub> Pd(NO <sub>2</sub> ) <sub>4</sub>	2.10	-	-	117	-	-	-	-	-	-	c
K <sub>2</sub> Pt(NO <sub>2</sub> ) <sub>4</sub>	2.02	-	-	-	-	-	-	-	-	-	c
DMG	-	-	-	-	-	1.27	1.27	115	-	1.44	c
Ethane	-	-	-	-	-	-	-	-	-	1.54	HB
Ethylene	-	-	-	-	-	-	-	-	-	1.34	HB
Benzene	-	-	-	-	-	-	-	-	-	1.39 <sub>5</sub>	HB

TABLE II. BOND LENGTHS AND BOND ANGLES (cont'd)

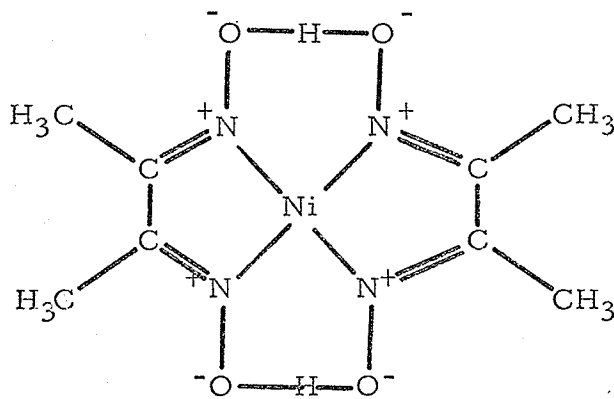
Compound	M-N distance	O-H-O distance	MNO bond angle	N-C distance	NCC bond angle	C-C	Ref.
Acetylene	-	-	-	-	-	1.20	HB
$\beta$ -diketone	-	-	-	-	-	1.49	HB
Paraffin							
4 coval. N	-	-	-	1.48	-	-	HB
3 coval. N	-	-	-	1.47	-	-	HB
Partial double bond: $(\text{HN} \overset{\text{H}}{\underset{\text{H}}{\text{C}}}=\text{O})_2$	-	-	-	1.32	-	-	b
Pyridine	-	-	-	1.35	-	-	b
Triple bond	-	-	-	1.16	-	-	b

and increase from the nickel to the palladium and platinum complexes; and none of these compounds have been conclusively shown to have symmetrical hydrogen bonds ( $\nu_{\text{OH}} = 2300 - 2900$ ) (19), although the oxygen-oxygen bond distance in  $\text{Ni}(\text{DMG})_2$  is short enough to suggest the existence of a single-minimum potential energy well. (3, 6, 19) Also this hydrogen on the bond is difficult to be replaced. The importance of metal-metal intermolecular interactions in the symmetrical planar complexes of nickel, palladium and platinum dimethylglyoximates (and even the heptoximates which are much less symmetrical) has been the subject of much dispute. Through X-ray (20), solubility (16, 21, 22) and dichroism (23) studies, Yamada and Tsuchida, Banks and Caton, Banks and Barnum, Godycki and Rundle had been able to say that metal-metal bonds do exist, with magnitudes of about 10 kcal / mole. (23) However, in more recent work, Basu, Cook and Belford (11), Anex and Krist (10) argued that the observed "abnormal" dichroism and comparatively low solubility of these compounds (which were taken as evidence for metal-metal bonding) might well be due to normal vibronic selection rules in a centric molecule and to crystal packing. Ingraham (24) undertook a theoretical molecular orbital treatment of nickel dimethylglyoximate using the extended Wolfsberg-Helmoltz method. He concluded that there is no evidence of metal-metal interaction in the ground state, but such interaction could happen in the excited states. The latest information obtainable was given by Thomas,

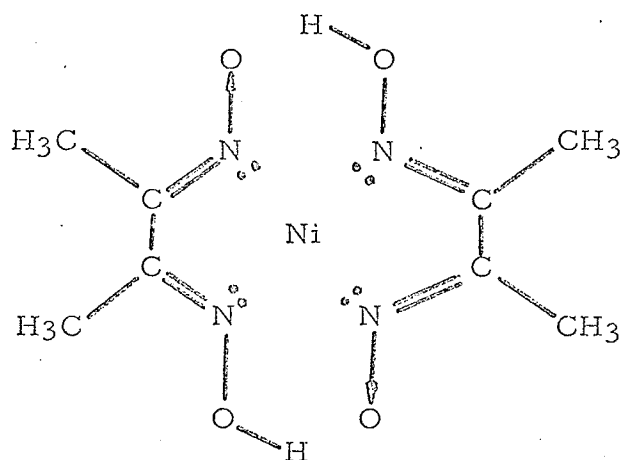
Underhill (25) and Bhat, Chaudrashekhar and Rao (26). Through a vibrating reed electrometer, they were able to detect semi-conductivity from these complexes ( $6.3 \times 10^{-15} \text{ ohm}^{-1} \text{ cm}^{-1}$  for  $\text{Ni}(\text{DMG})_2$  and  $8.9 \times 10^{-12} \text{ ohm}^{-1} \text{ cm}^{-1}$  for  $\text{Pd}(\text{DMG})_2$ , both at  $100^\circ\text{C}$ ). And Thomas and Underhill claimed their measurements to be the first direct evidence for electron delocalization along the line of metal-metal stacking. No evidence of metal-metal bonding would be expected from mass spectral studies since the high energy of electron impact will be too great to preserve this weak bond, if it ever existed. As can be seen from table II, complexing the metal with the vic-dioximes in every instance results in formation of rather strong metal-nitrogen bonds, as evidenced by the short bond lengths ( $1.85 \text{ \AA}$  for  $\text{Ni}(\text{DMG})_2$  and  $1.96 \text{ \AA}$  in  $\text{Pt}(\text{DMG})_2$  as compared to  $2.12 \text{ \AA}$  in triethylenediamine-Ni(II)-nitrate,  $\text{Ni}(\text{en})_3(\text{NO}_3)_2$ ). Also the C-C bond between the dioxime (NOH) groups is increased from  $1.44 \text{ \AA}$  in the free ligand to  $1.50 \pm 0.03 \text{ \AA}$  in the complexes, reflecting probably a "pull-over" of the little double bond character of the carbon-carbon bond through the carbon-nitrogen bonds to the metal-nitrogen bonds. Complexation decreases the carbon-nitrogen bond length in the case of nickel dimethylglyoximate ( $1.27 \text{ \AA} \longrightarrow 1.23 \text{ \AA}$ ) and increases it in the case of palladium and platinum dimethylglyoximates ( $1.27 \text{ \AA} \longrightarrow 1.31 \text{ \AA}$  and  $1.38 \text{ \AA}$  respectively.) The C-C bond ( $1.47 - 1.57 \text{ \AA}$ ) is longer than the aromatic C-C bond ( $1.395 \text{ \AA}$  in copper acetylacetonate,  $1.404 \text{ \AA}$  in benzene) and encompasses

that of a normal C-C single bond ( $1.54 \overset{\circ}{\text{A}}$  in ethane). Thus, there appears to be some conjugation through the metal-nitrogen-carbon bonds to give each of these bonds some double-bond character, but the C-C bond seems to have little double-bond character. This was postulated by Godycki and Rundle from their X-ray studies and supported by Banks and Barnum (22) through their studies of the absorption spectra of some of these vic-dioximates. Additional maxima at 435  $\mu$  and 406  $\mu$  (for  $\text{Ni}(\alpha\text{-DFD})_2$  and  $\text{Ni}(\text{DPG})_2$  respectively) were observed with respect to those observed for  $\text{Ni}(\text{Niox})_2$ ,  $\text{Ni}(4\text{MNiox})_2$ ,  $\text{Ni}(\text{DMG})_2$  and nickel heptoximate. They attributed these additional peaks to conjugation of the vic-dioxime groups with the aromatic groups. They found a similar effect with the palladium complexes.

The molecular structure given by Godycki and Rundle (7) is



with a symmetry which may be as high as  $D_{2h}$ . The four positive charges lie on the nitrogen atoms, and are neutralized by the oxygen atoms. Hückel preferred the following form :



This would also give the nickel atom a very strong stable electronic configuration and ensure four very strong M-N bonds. In view of the five electrons present in the electron-donor nitrogen atom, covalency seems to be rather appropriate for the M-N bonds. This nature of covalency for the M-N bonds had been proposed by Banks (21) for  $Ni(DMG)_2$  from his charge transfer absorption spectra studies. However, there is still a lack of knowledge as to how the metal and ligand orbitals are mixed when we consider the problem from the molecular orbital calculation point of view. (10)

From the mass spectral study of these complexes, it is hoped that a little more about the bonding can be said.

CHAPTER TWO  
THERMOGRAVIMETRIC ANALYSIS

## SECTION I. INTRODUCTION

Thermogravimetric analysis (TGA) together with other techniques such as differential thermal analysis (DTA) and gas evolution detection (GE or GED) are not new thermoanalytical methods, but it is only in recent years have they become highly developed research tools. TGA has been employed in the studies of such various physicochemical aspects such as thermal stability temperatures, dissociation intermediates, thermal stability of intermediates, residue composition and kinetics. (28) And Honda (29), Newkirk (30, 31), Duval (32) and Wendlandt (33) have been especially noted for their contribution to this field. However, the literature concerning thermal analysis contains many contradictions and anomalies. The shape of a thermogram can depend on so many factors such as sample size, state of subdivision, how tightly the sample is packed in its container, shape of the container, rate of heating, ambient atmosphere and detection device. (31) Other effects like thermo-molecular flow, aerodynamics and temperature coefficient can be important too, especially when the experiment is carried out in vacuum. The thermogram of calcium oxalate, for example, has often been used as a standard for thermobalance operation yet it has been shown that the shape of the thermogram is dependent on so many of these factors. The effect of some of these variables is greater with large samples than with small samples. Commonly samples as large as 0.5 - 1.0 gram have been used in the

recent past. The highly sensitive Cahn balance used here allowed reproducible results to be obtained with samples as small as 1mg. For these small samples, the effect of temperature gradients within the sample should be minimal but many of these other variables can still be operative.

The thermolysis of some of the vic-dioximates was first studied by Duval (32) but with the advent of new highly developed thermobalances, a renewed study of them is necessary. The thermal stability of them has to be known first before the interpretations of their mass spectra are justified.

## SECTION II. INSTRUMENTAL - THE THERMAL BALANCE

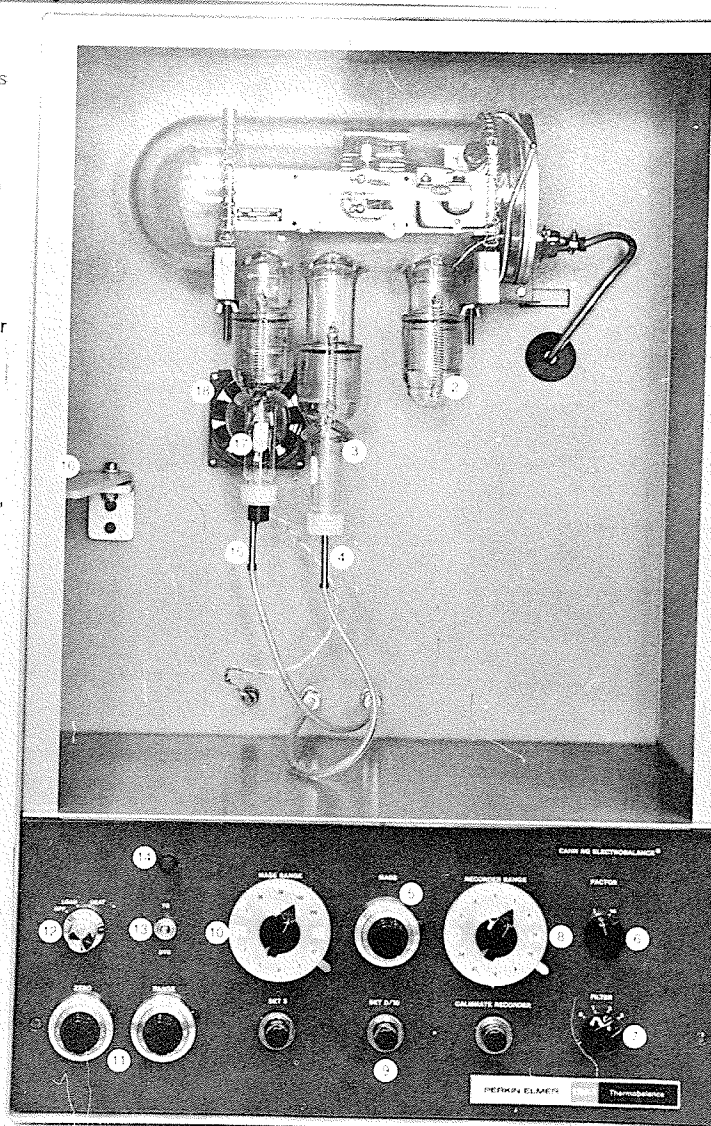
The thermal balance used here is the Perkin - Elmer TGS - 1 model (fig 1). The main components are shown alongside the diagram. It provides a record of microgram level weight changes in the sample as a function of temperature while it is being heated. The temperature is controlled through a temperature programmer in a differential scanning calorimeter (Perkin - Elmer DSC - 1 B type) connected to the TGA - 1. The main components are described in the following. (34)

(a) The Cahn RG Automatic Electrobalance works on the null-balance principle. (35) A change in weight of the sample in the sample pan in loop A (or loop B) will cause a deflection of the beam. The flag at the end of the beam will move with it, changing the light

FIG. 1

THERMOBALANCE COMPONENTS  
OF MODEL TGS-1

- 1 CAHN RG Electrobalance
- 2 Counterweights
- 3 Hangdown tube for high mass ranges
- 4 Sweeping gas inlet
- 5 Mass dial—ten-turn precision potentiometer for mass determination—reads percent of Mass Range setting
- 6 Factor selector—to reduce Recorder Range by a factor of ten if desired
- 7 Noise filter selector
- 8 Recorder Range—Portion of balance range displayed full scale on recorder
- 9 Balance and recorder mass calibration controls
- 10 Mass Range—balance range in mgs.
- 11 Temperature calibration controls
- 12 Selector switch, OFF, LOAD (balance on, heater off), and HEAT (balance on, heater on)
- 13 Selector switch, normal integral mode, TG; and differential mode, DTG
- 14 Dual intensity pilot light—dim indicates system is on but not in temperature control, bright indicates system is in temperature control
- 15 Sweeping gas outlet
- 16 Supporting arm for magnet
- 17 Micro Furnace surrounding sample
- 18 Fan



intensity incident on the phototubes. This will then give a different reading in the phototube current. This current, after being amplified, is applied to the coil attached to the beam. The beam is in a magnetic field and the whole set-up is similar to that of a dc-motor. The current on the beam thus exerts a restoring force

$$F = i b B \quad (1)$$

where  $i$  = current in amps.

$b$  = width of loop in cm.

$B$  = magnetic field strength in oested

attempting to put the beam back to its original position. This change in the electromagnetic force is equal to the change in weight. A schematic diagram of the thermobalance is shown in fig. 2.

(b) The furnace comprises a platinum heating element embedded in a ceramic cylinder for heating the sample (or standard). The furnace is supported from below by a suitable length of ceramic rod, with the heating coil connections going through it, onto the base of a plug which can be screwed onto the bottom of the hang-down tube.

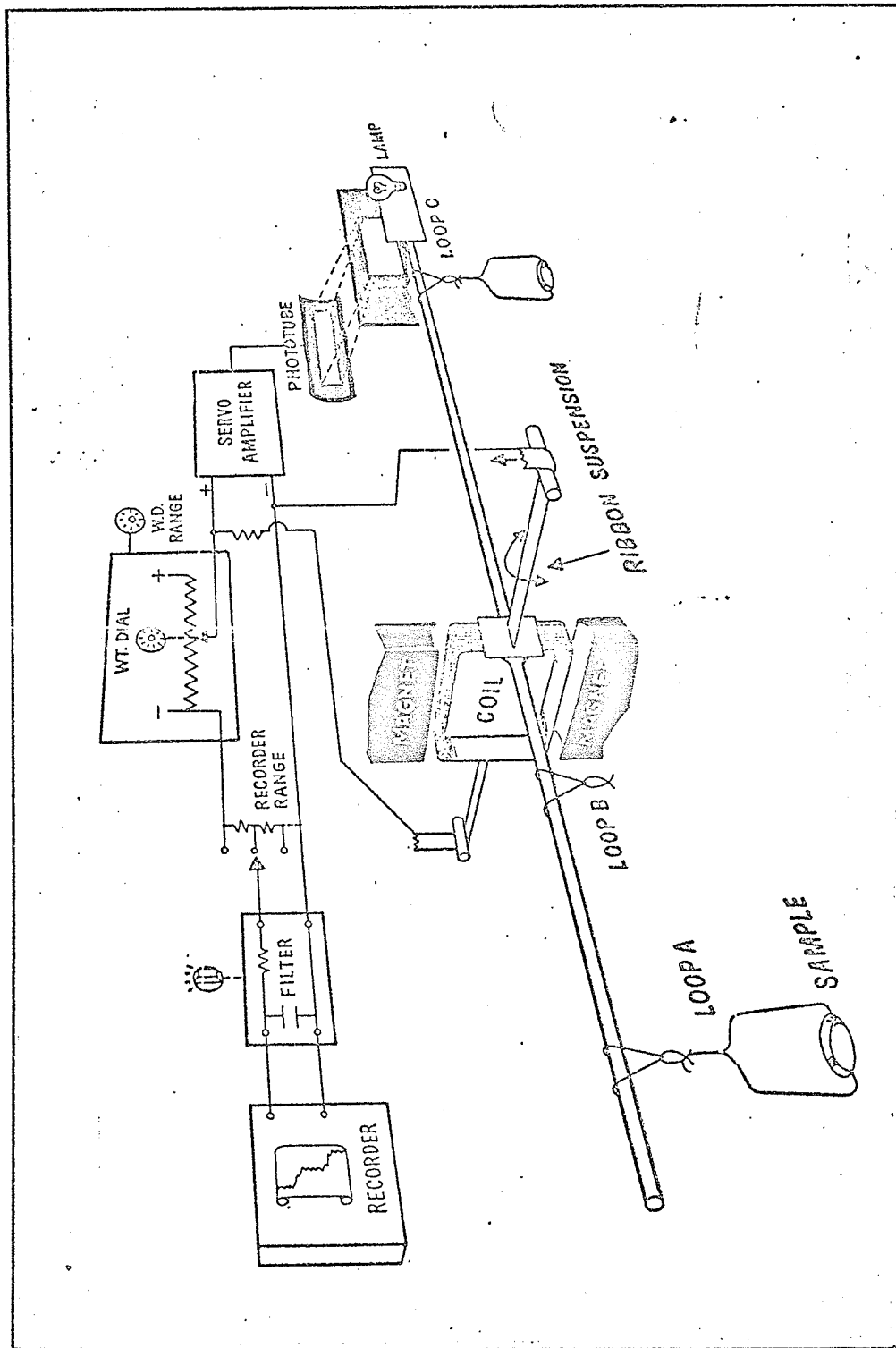
(c) The electronic control unit which consists of all the various units for zeroing, calibrating and weighing mechanisms. They are :

Power switch for OFF, and ON for loading and heating.

MASS RANGE in two groups of mass values ( 1 - 200 mg.

FIG. 2

SCHEMATIC DIAGRAM OF CAHN RG  
AUTOMATIC ELECTROBALANCE



for loop A and 5 - 1000 mg. for loop B).

MASS which permits a 4-digit reading of the sample weight and is used in liasion with the MASS RANGE. It can be used for both zeroing and measuring procedures.

RECORDER RANGE which is really a sensitivity control.

FACTOR, a two-position scale expansion control with factors 1 and 10. It multiplies the recorder reading - RECORDER RANGE setting product.

SET 5 and SET 0/10 which are used for zeroing the recorder.

CALIBRATE RECORDER which is used to set pen at 100% after zeroing procedure is completed.

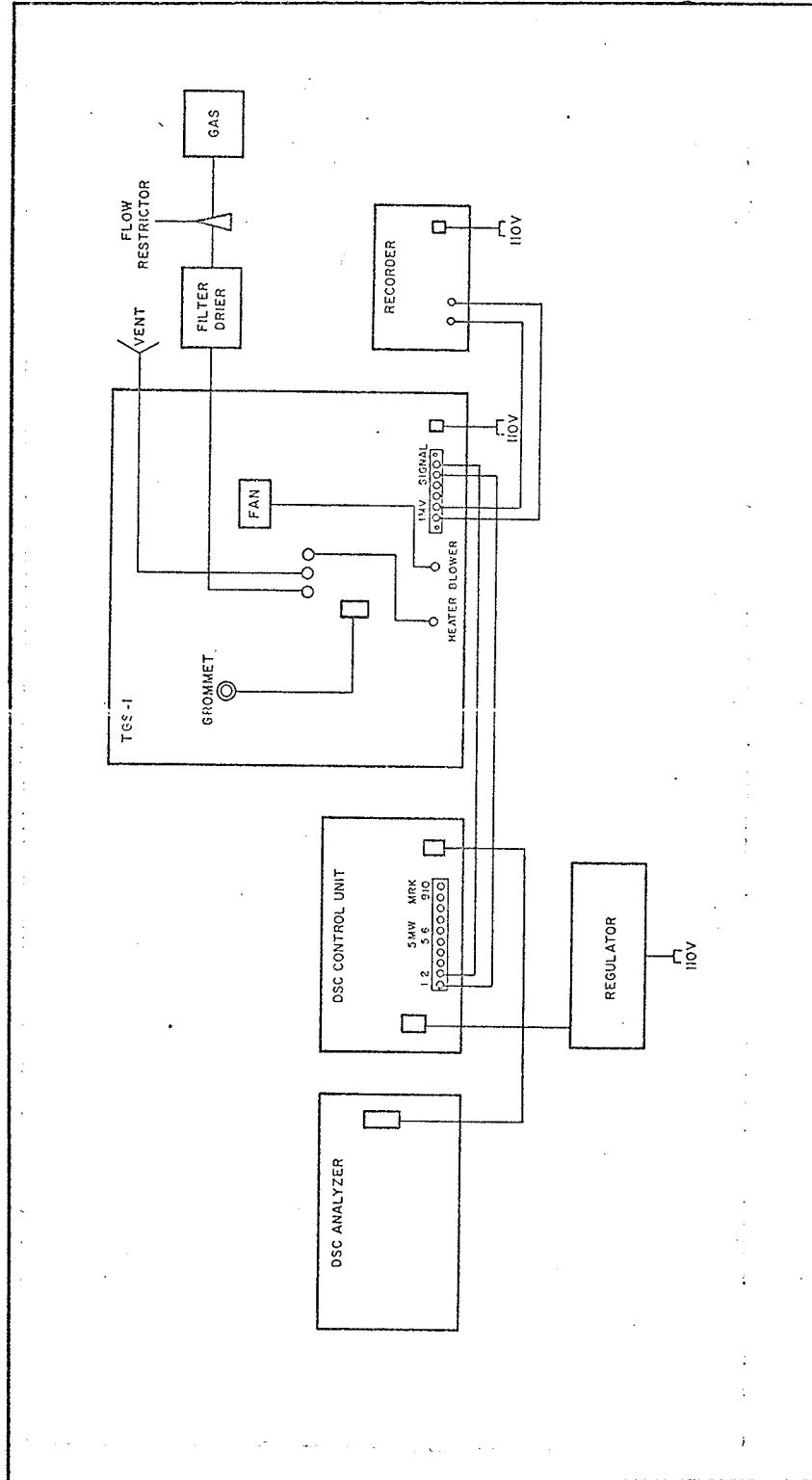
FILTER which is used for damping purposes.

ZERO which is used to regulate the power supply to the furnace during calibration with the ferromagnetic standards. The change per turn of the dial is linear and it gives approximately  $10^{\circ}\text{C}$  per revolution.

RANGE which is used to the same effect as the ZERO control except that the change produced is not linear. It is about  $0.9^{\circ}\text{C}$  per unit division change in the dial at the higher temperature range ( $400^{\circ} \pm 100^{\circ}$ ) and  $0.3^{\circ}\text{C}$  at the lower range ( $200^{\circ} \pm 100^{\circ}$ ). A schematic diagram of the electrical and gas connections is shown in fig 3.

FIG. 3

ELECTRICAL AND GAS CONNECTIONS  
OF THERMOBALANCE SET - UP



SECTION III. EXPERIMENTAL - SAMPLE PREPARATION  
AND INSTRUMENT CALIBRATION

(a) SAMPLE: All the nickel dioximates were prepared by dissolving the appropriate dioxime in alcohol and adding an aqueous solution of nickel chloride to it. There was immediate precipitation of the metal-chelate in every case. The precipitate was filtered off, washed thoroughly with alcohol and then dried in an oven at about  $60^{\circ}\text{C}$ .

The palladium complexes were prepared by adding a  $\text{Pd}^{+2}$  solution to an alcohol dioxime solution. The  $\text{Pd}^{+2}$  solution was made by heating palladous chloride in water to which a few cc. of hydrochloric acid had been added. Any residue was filtered off.

The platinum complexes were prepared in a similar way to the palladium complexes. The  $\text{Pt}^{+2}$  solution was obtained by dissolving potassium chloroplatinite  $\text{K}_2\text{PtCl}_4$ . The colours of the complexes are shown in table III.

The change in weight of the compounds during heating was recorded as percentage change on a Texas Instruments Incorporated Reading Data model Servo / Riter WD chart recorder.

(b) CALIBRATION of the instrument for accurate temperature read-out was undertaken by use of the magnetic standards, namely, alumel, mumetal, microseal, perkalloy and iron. A small sample of each of these (total weight less than or equal to one mg.) was

TABLE III. MOLECULAR WEIGHTS AND COLOUR OF THE METAL VIC-DIOXIMATES

complexes oximes		Ni	Pd	Pt	Refs.
Dimethyl- glyoxime	1.	brick red	yellow	bronze	4, 5, 6
	2.	brick red	yellow	bronze	
	3.	288	336	425	
Diphenyl- glyoxime	1.	orange	yellow	green	4, 5
	2.	orange	yellow	pink-red	
	3.	536	584	673	
Difuril- dioxime	1.	red	orange	red-bro.	4
	2.	or. -red	orange	red-bro.	
	3.	496	544	633	
Nioxime	1.	scarlet	yellow	grey	4
	2.	scarlet	yellow	grey	
	3.	340	388	477	
4-methyl- nioxime	1.	scarlet	-	grey-bl.	4
	2.	scarlet	yellow	grey-bl.	
	3.	368	416	505	

1. Literature citing
2. Obtained in this work
3. Molecular weight of the respective complexes
4. C. V. Banks and D. W. Barnum, J. A. C. S. 80, 4767 (1958)
5. S. C. Ogburn, J. A. C. S., 48, 2493 (1926)
6. A. G. Sharpe and D. B. Wakefield, J. C. S. 281 (1957)

heated together in the sample pan under conditions similar to those used in the thermogravimetric analysis experiments, and under the influence of the magnetic field of a small magnet. Each standard has its own particular Curie point. As the temperature of the sample passes through the Curie temperature of one of the metals, an apparent weight loss occurs and this is recorded on the chart paper, where a comparison can be made with the temperature recorded by the temperature marking pen. The ZERO and RANGE dials were adjusted after each run until a satisfactory agreement between the apparent temperature readings and the manufacturer's stated values of these standards was obtained. It was not possible to achieve perfect agreement over the whole temperature range of the instrument and the best compromise settings were sought. This occurred when the thermobalance controls were set at ZERO = 555 and RANGE = 350 and these settings were used in all subsequent experiments. The results are shown in table IV. The machine was not accurately calibrated for use above  $650^{\circ}\text{C}$  and definitely temperatures above  $800^{\circ}\text{C}$  are unreliable. Experiments carried out here seldom exceeded  $650^{\circ}\text{C}$  in air and  $800^{\circ}\text{C}$  in nitrogen. As a matter of fact, unreliable results would be produced above  $800^{\circ}\text{C}$  since above this temperature, the nichrome hangdown wire and stirrup probably were being oxidised. The platinum pan might not have been affected. Fig. 4 shows a gradual weight-gain after  $700^{\circ}\text{C}$  when the empty sample pan is heated in air and no

TABLE IV. COMPARISON OF APPARENT AND MANUFACTURER'S VALUES OF CURIE POINTS OF MAGNETIC STANDARDS USED

	Manufact. values	Apparent Expt. val	Difference
Alumel	158	158	0
Mumetal	390	394	+4
Nicroseal	445	444	-1
Perkalloy	598	602	+4
Iron	786	770	-16

FIG. 4

EFFECT OF HEAT ON STIRRUP,  
HANGDOWN WIRE AND SAMPLE  
PAN OF THERMOBALANCE IN  
AIR, NITROGEN AND VACUUM

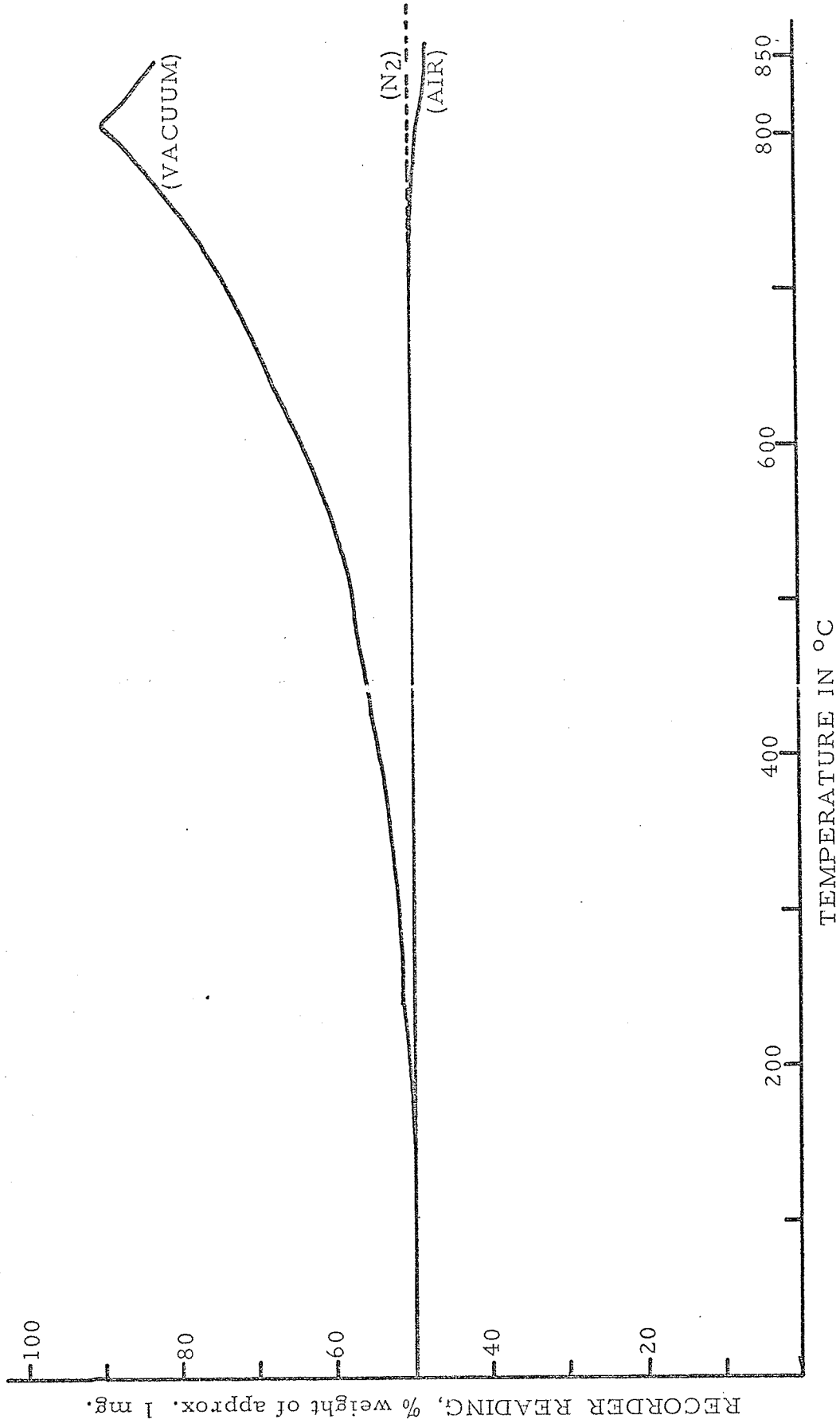


FIG. 4 EFFECT OF HEAT ON STIRRER, HANGDOWN WIRE AND SAMPLE PAN OF THERMOBALANCE IN AIR, NITROGEN, AND VACUUM.

apparent weight-gain when the ambient atmosphere is nitrogen. The same figure shows the effect of heating the empty sample pan in vacuum. This apparent weight-loss is probably due to thermomolecular flow. Thus corrections to thermograms are required for later experiments performed in vacuum.

(c) TGA MODE ANALYSIS : A sample weight of approximately 1 mg. was used in each case. A heating rate of  $10^{\circ}\text{C}$  per minute was used in general and other rates and sample weights were used as such need arose. A RECORDER RANGE of 0.1 was used except where otherwise stated. The weight of the stirrup, hangdown wire and platinum sample pan was set at 0% weight on the recorder chart. Sample was added to the pan to make the pen read 100% (or very close to it). This would be equivalent to a sample weight of approximately 1 mg. The heater was turned on and the sample was heated to the desired temperature at the required heating rate.

In running the experiment in a nitrogen atmosphere, a steady stream of nitrogen at a low flow-rate of 20 ml. per min. was passed through the apparatus. This nitrogen was dried beforehand by passing it through a filter-drier containing silica gel. The sample was weighed in air and nitrogen was passed through the apparatus for twenty minutes. The flow of nitrogen caused an apparent change of sample weight. The recorder pen was adjusted to its original position before the furnace heaters were switched on. Since the thermal conductivity of both nitrogen and air are the

the same, no error in weight would be caused by this readjustment procedure.

(d) DTG MODE ANALYSIS : All samples were run with a more sensitive scale of RECORDER RANGE = 0.04 instead of 0.1.

Other specifications were the same as in the TGA mode, i. e. scan rate of 10°C per min. , ZERO at 555 and RANGE at 350.

#### SECTION IV. RESULTS AND DISCUSSIONS

The thermograms of the complexes obtained under various conditions are shown in figs. 5 - 19.

Some preliminary comments can be made about the thermograms. All complexes are stable up to at least 250°C, as shown by the horizontal plateaux in the initial part of the thermograms. In some cases, small weight losses of 1 - 2% were observed which may be due to slight sublimation or loss of small amounts of volatile impurity or complex. When decomposition does occur, it occurs much more rapidly in the presence of oxygen than in a nitrogen atmosphere or vacuum (as shown in the cases of diphenylglyoximates and  $\alpha$ -furildioximates, figs. 20, 21). All decomposition temperatures for runs in nitrogen are higher than those obtained from runs in air. (table V). This lowering in temperature and greater extent of decomposition for the runs in air clearly demonstrate the exothermic nature of the process. This thermo-oxidation of the metal or ligand or both raises the temperature

TABLE V. DECOMPOSITION TEMPERATURES OF  
VIC - DIOXIMATES

COMPLEX	DTG, in °C 10°/min.	Duval's Results	TGA TEMPERATURE				
			AIR, 5°/min.	10°/min.	20°/m.	40°/m.	N <sub>2</sub> , 10°/m.
Ni(DMG) <sub>2</sub>	338	250	-	334	-	-	340
Pd(DMG) <sub>2</sub>	332	228	-	330	-	-	354
Pt(DMG) <sub>2</sub>	332	-	-	336	-	-	332
Ni(DPG) <sub>2</sub>	362	no	342	362	-	-	362
	402		382	406	-	-	-
Pd(DPG) <sub>2</sub>	384b	-	348	372	386	392	338
	-		-	384	402	414	-
Pt(DPG) <sub>2</sub>	328	-	324	340	-	-	388a
Ni(α-DFD) <sub>2</sub>	304	no	298	304	-	-	314
	334		312	330	-	-	340
	422		384	398	-	-	-
Pd(α-DFD) <sub>2</sub>	318	-	316	316	-	-	318
	338		340	360a	-	-	-
	382		384	-	-	-	-
Pt(α-DFD) <sub>2</sub>	330	no	302	304	-	-	330
Ni(Niox) <sub>2</sub>	300	115	-	298	-	-	314
Pd(Niox) <sub>2</sub>	282	169	-	270	-	-	320
Pt(Niox) <sub>2</sub>	262	-	-	260	-	-	300a
Ni(4MNiox) <sub>2</sub>	282	-	284	284	-	-	302a
Pd(4MNiox) <sub>2</sub>	266	-	260	264	-	-	314
Pt(4MNiox) <sub>2</sub>	270	-	240	270	-	-	286a

a.-temperature obtained at junction of two tangents (one to the start of decomposition and the other to the final decomposition process)

b.-temperature taken at maximum decomposition

no - no decomposition temperature obtainable

FIGS. 5 - 19

THERMOGRAMS OF VIC -  
DIOXIMATES OBTAINED UNDER  
VARIOUS HEATING RATES AND  
AMBIENT ATMOSPHERES

SPECIFICATIONS :

----- 5<sup>o</sup>/ min. in air

———— 10<sup>o</sup>/ min. in air

⊙⊙⊙⊙ 20<sup>o</sup>/ min. in air

×××× 40<sup>o</sup>/ min. in air

..... 10<sup>o</sup>/ min. in nitrogen

..... 10<sup>o</sup>/ min. in nitrogen + air

———— 10<sup>o</sup>/ min. in DTG experiements

Recorder Range = 0.04 for DTG runs

Recorder Range = 0.10 for all other runs

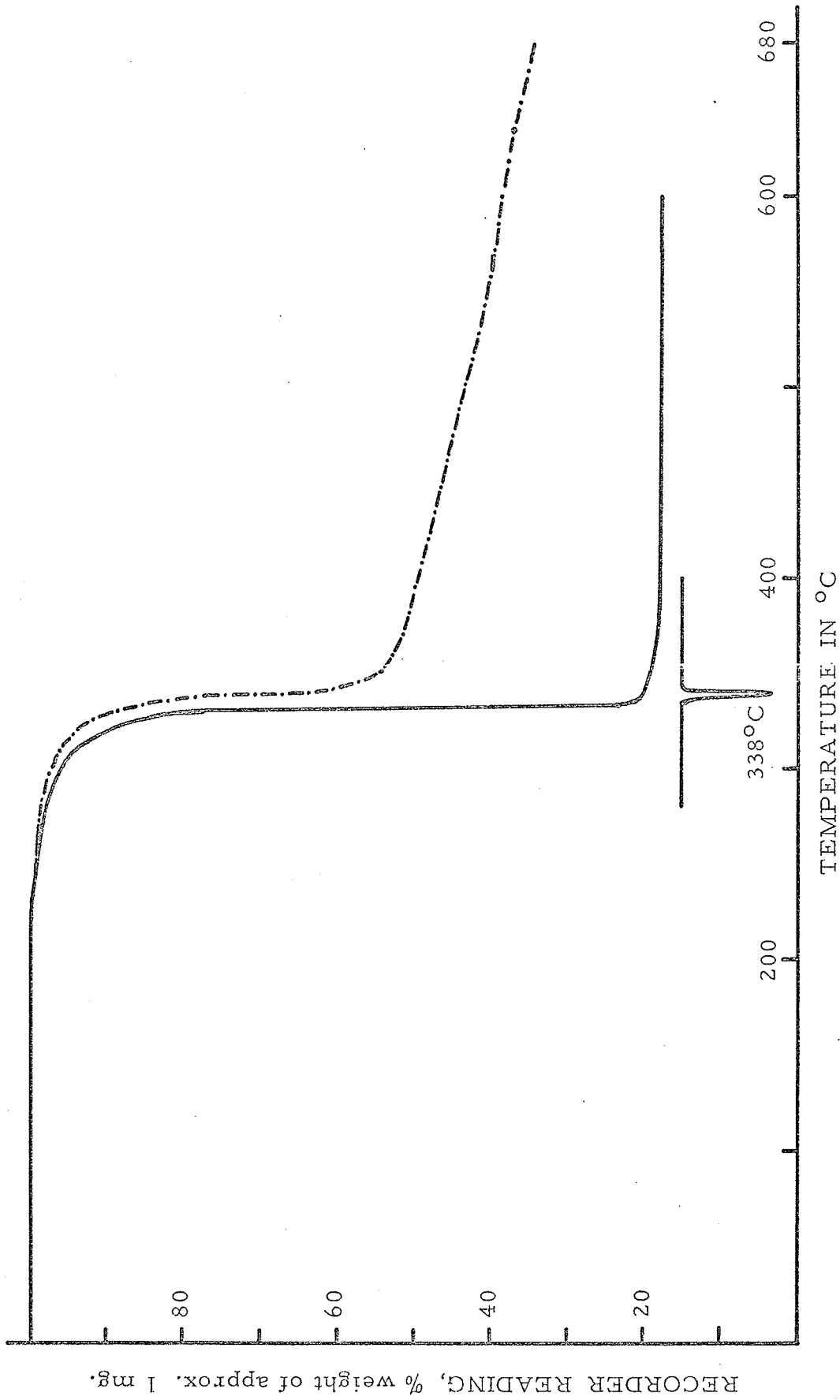


FIG. 5 THERMOGRAM OF Ni(DMG)<sub>2</sub>

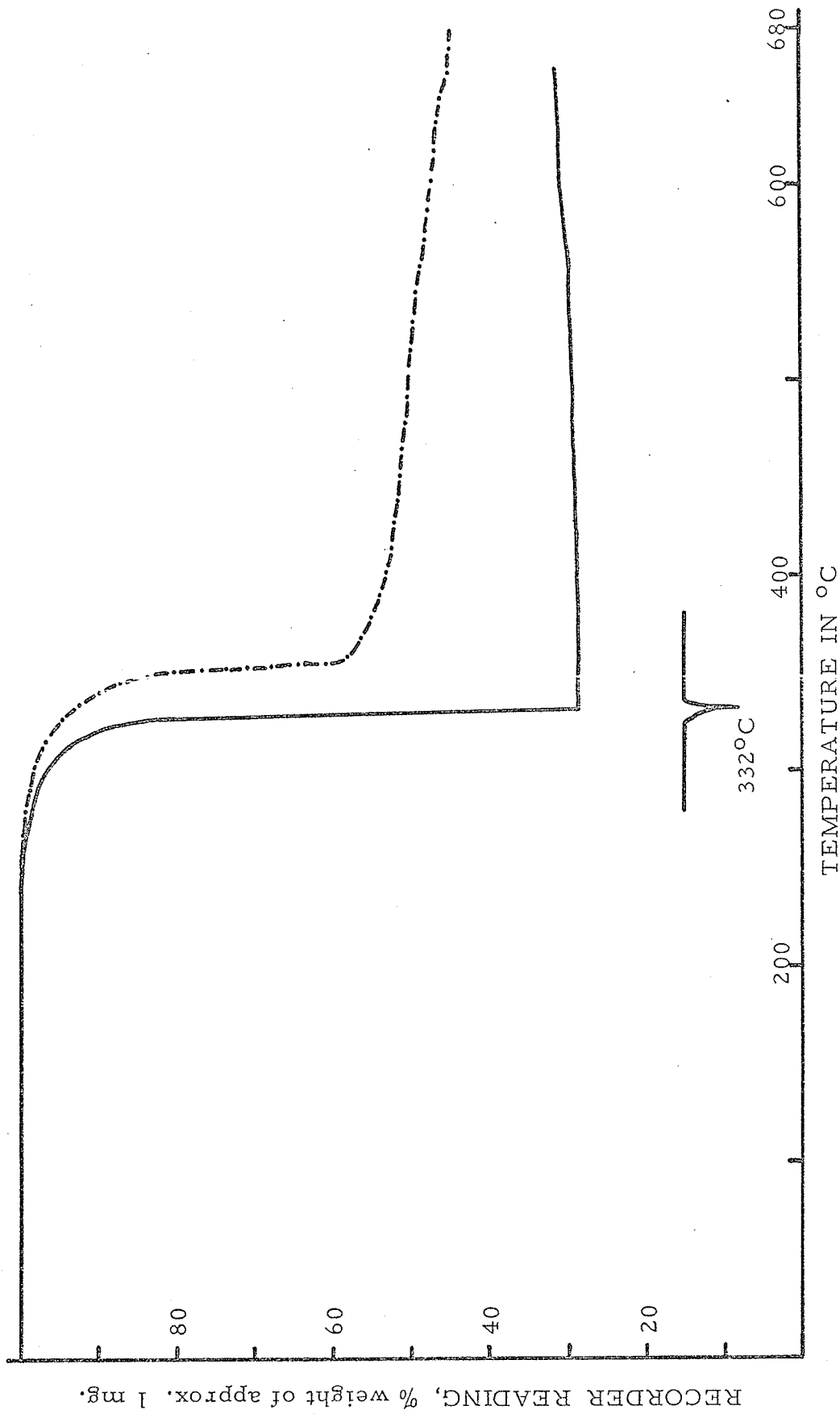


FIG. 6 THERMOGRAM OF Pd(DMG)<sub>2</sub>

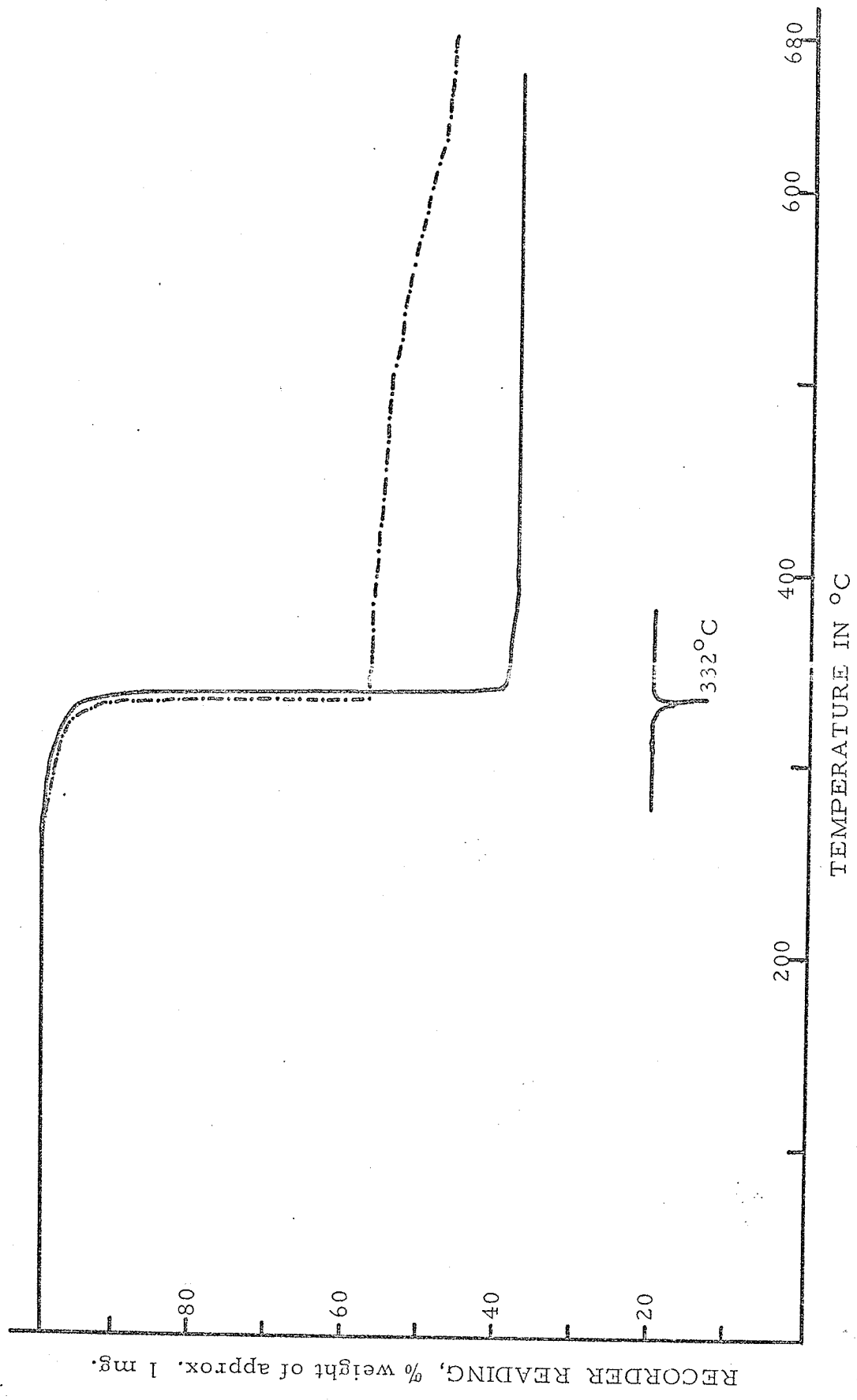


FIG. 7 THERMOGRAM OF Pt(DMG)<sub>2</sub>

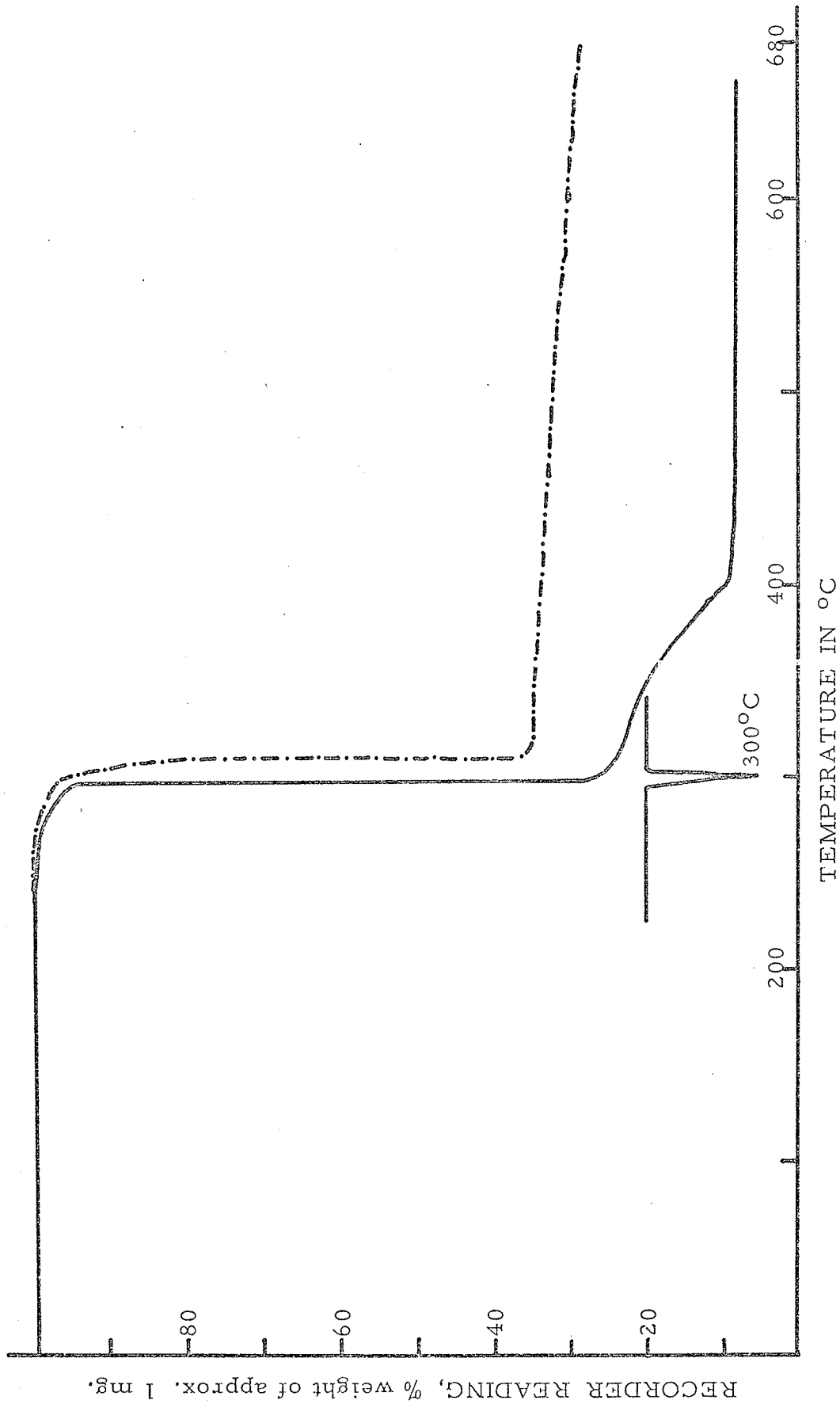


FIG. 8 THERMOGRAM OF  $\text{Ni}(\text{NiOx})_2$

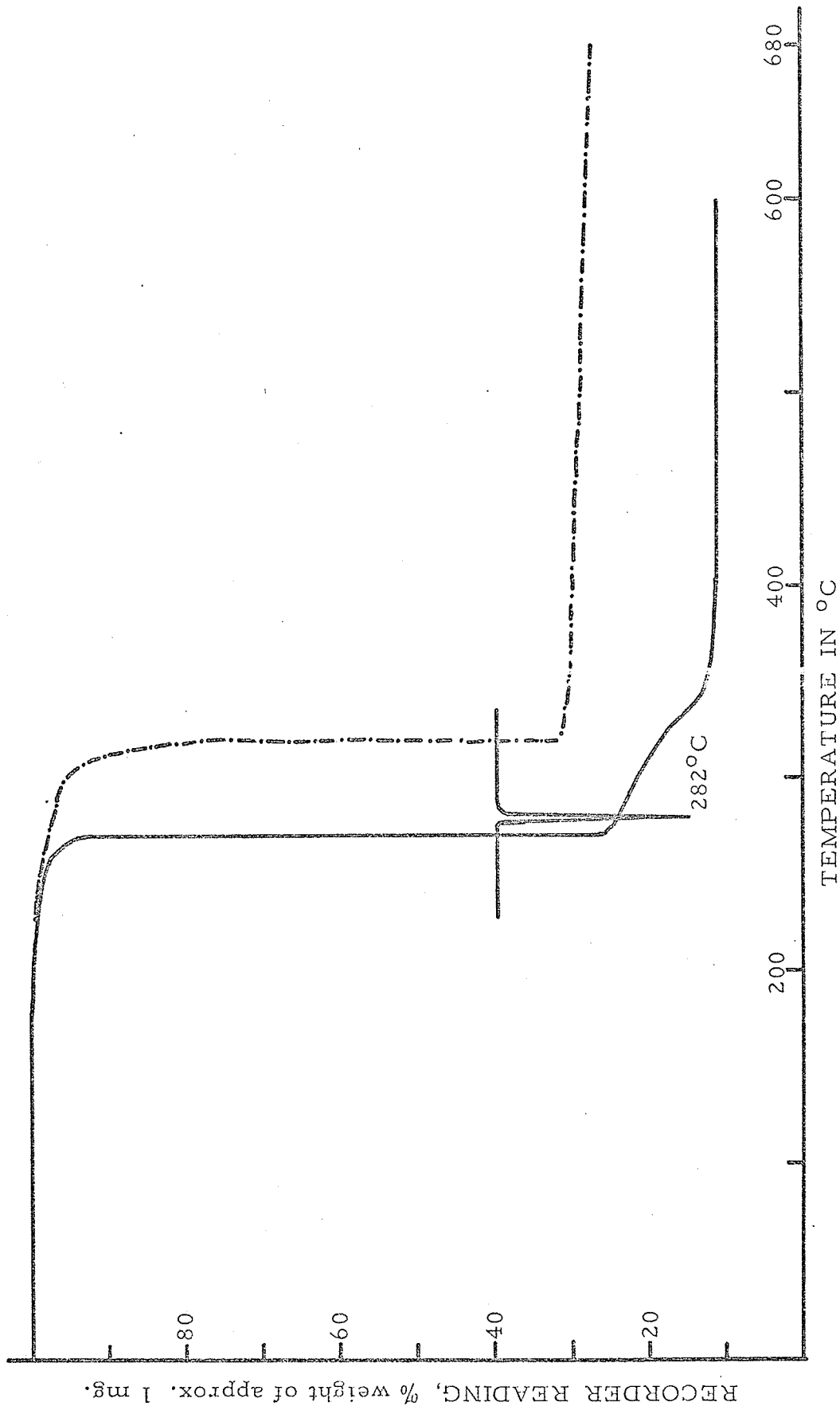


FIG. 9 THERMOGRAM OF Pd(Niox)<sub>2</sub>

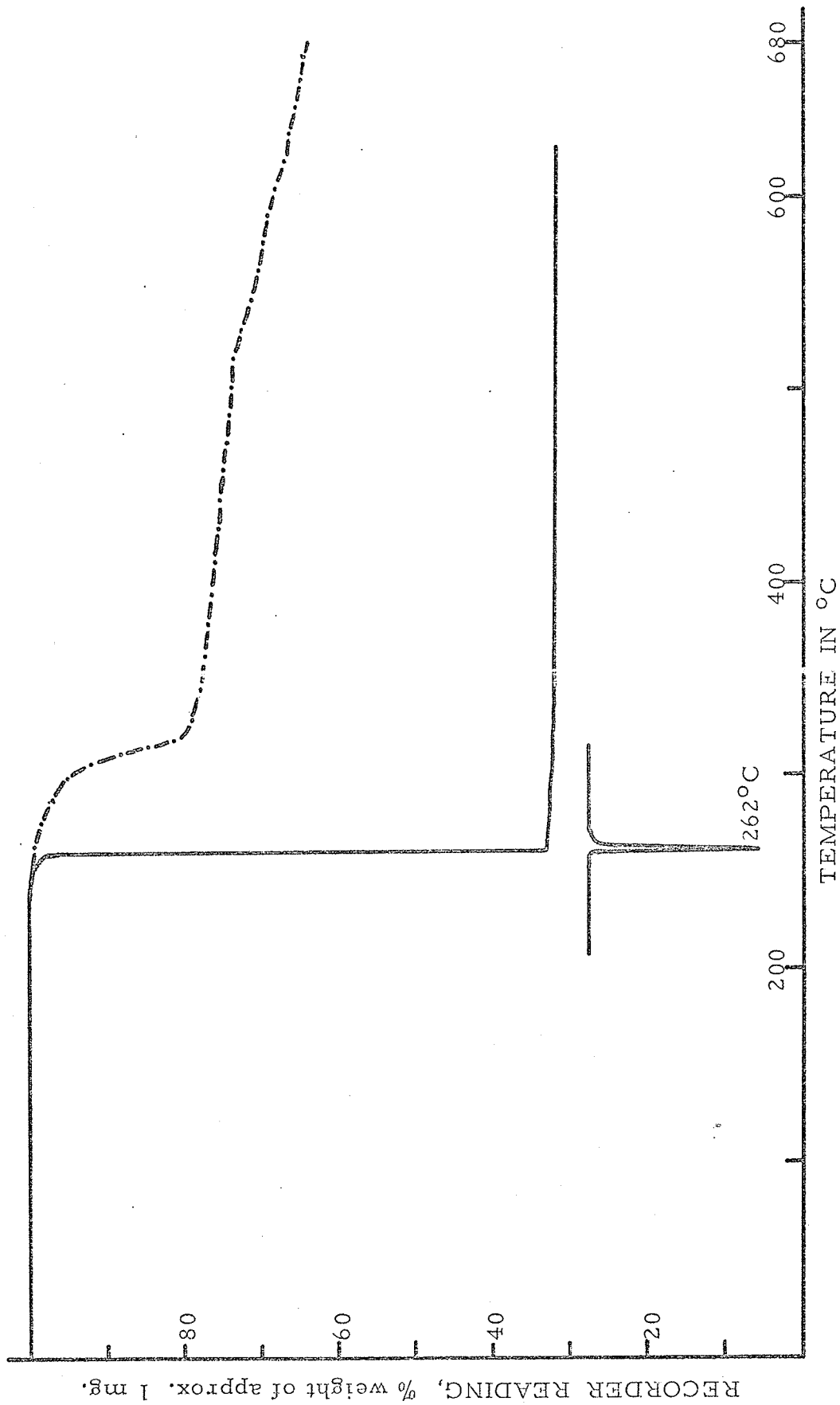


FIG. 10 THERMOGRAM OF Pt(NiOx)<sub>2</sub>

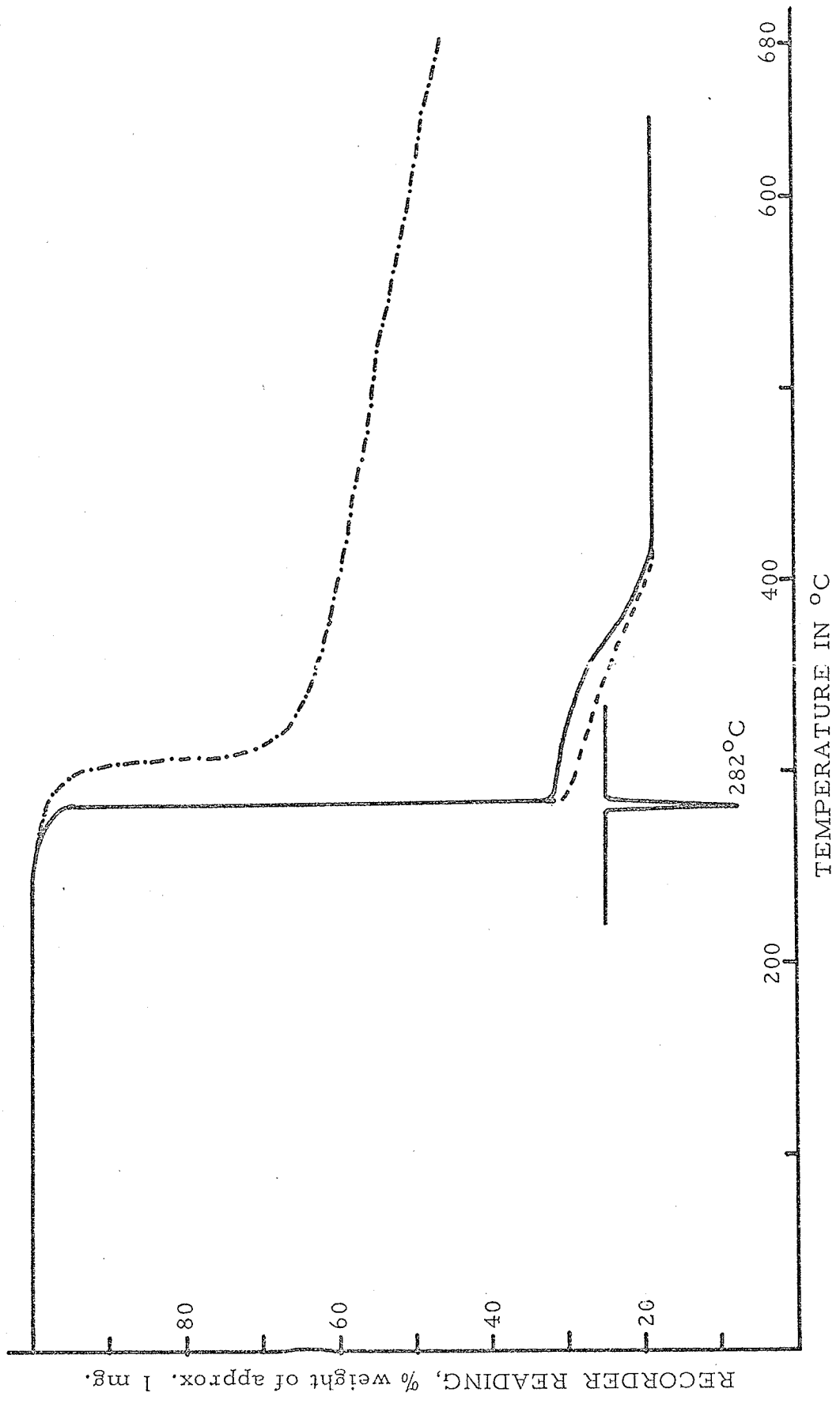


FIG. 11 THERMOGRAM OF Ni(4MNiox)<sub>2</sub>

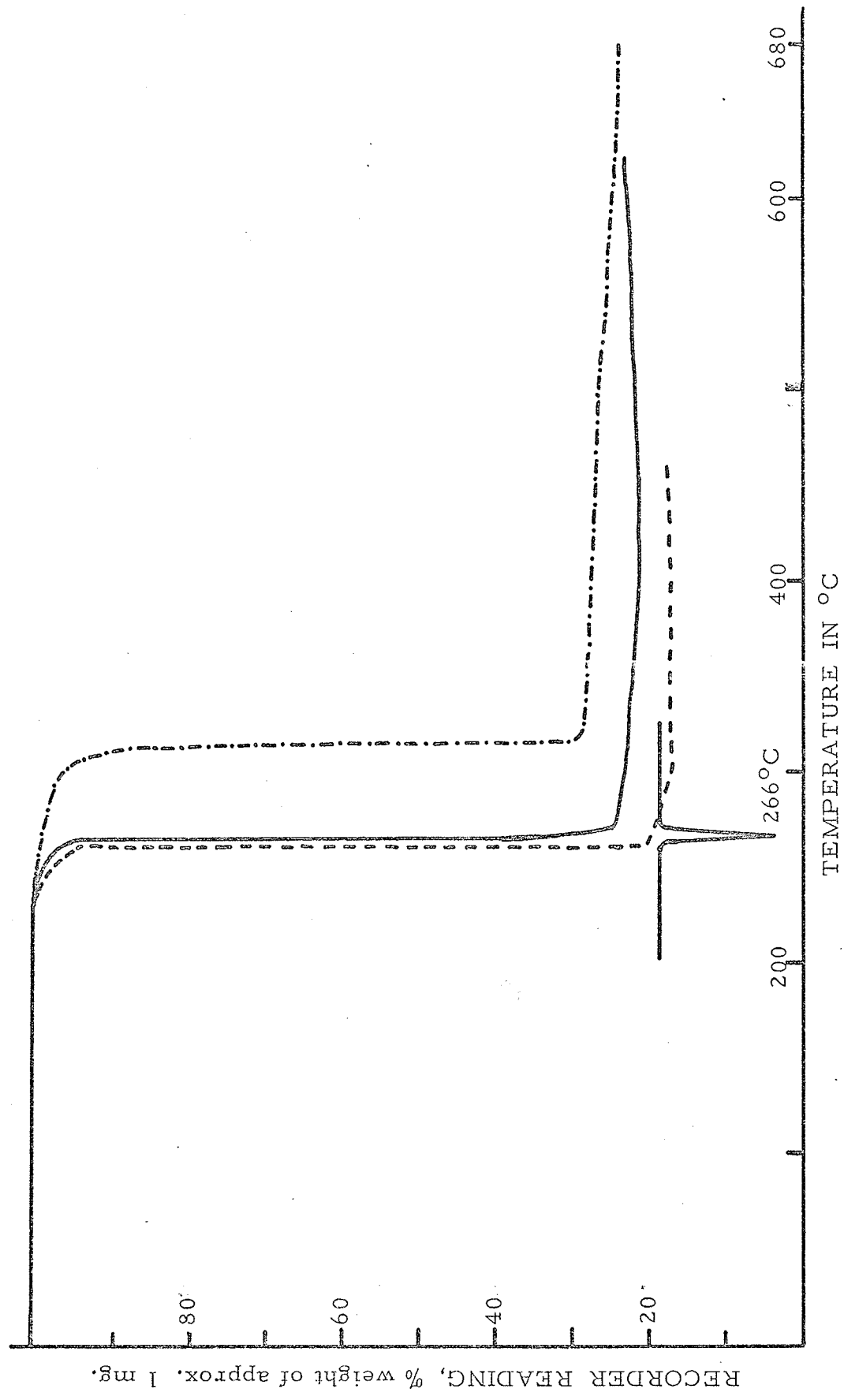


FIG. 12 THERMOGRAM OF Pd(4Mniox)<sub>2</sub>

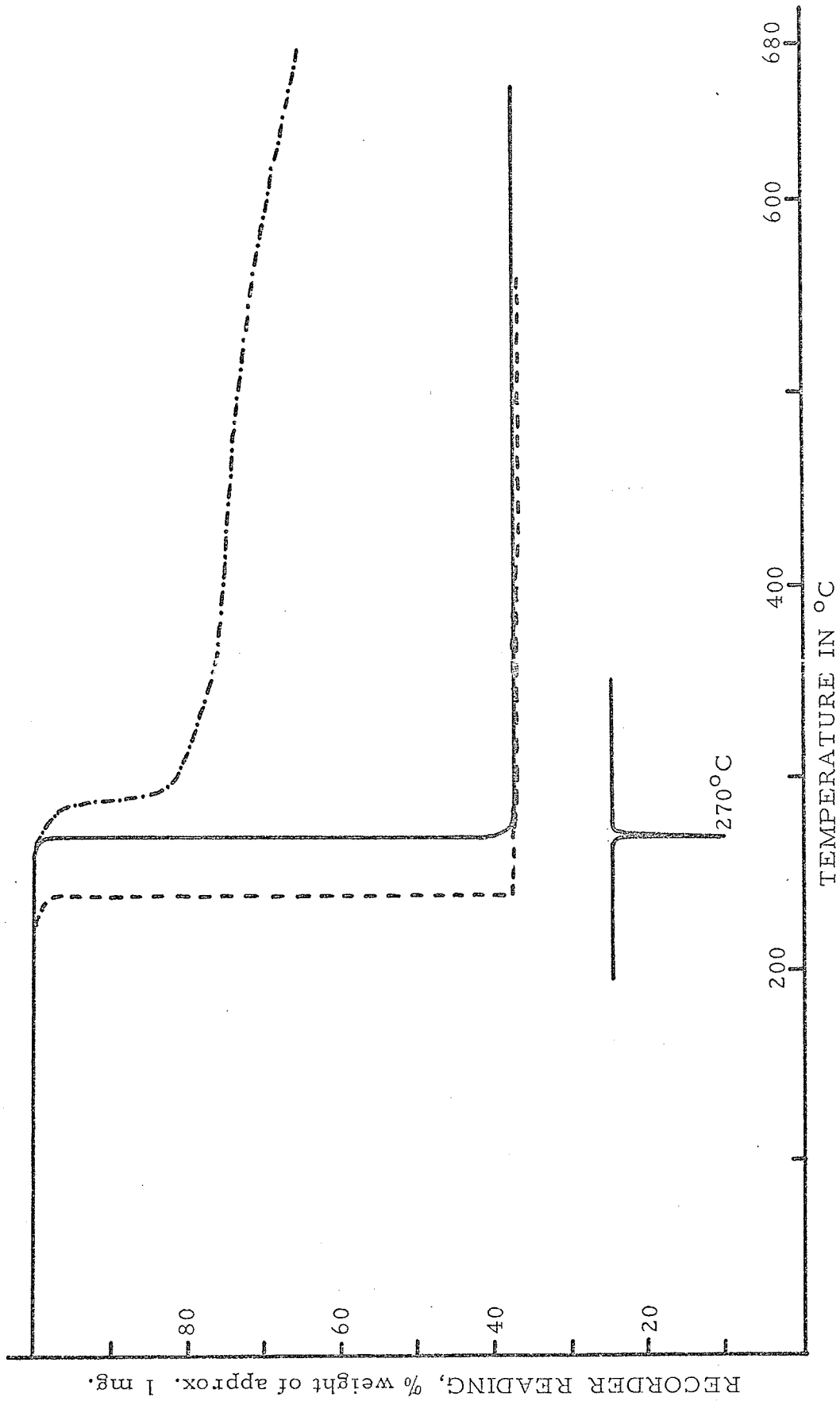


FIG. 13 THERMOGRAM OF  $Pt(4MNiOx)_2$

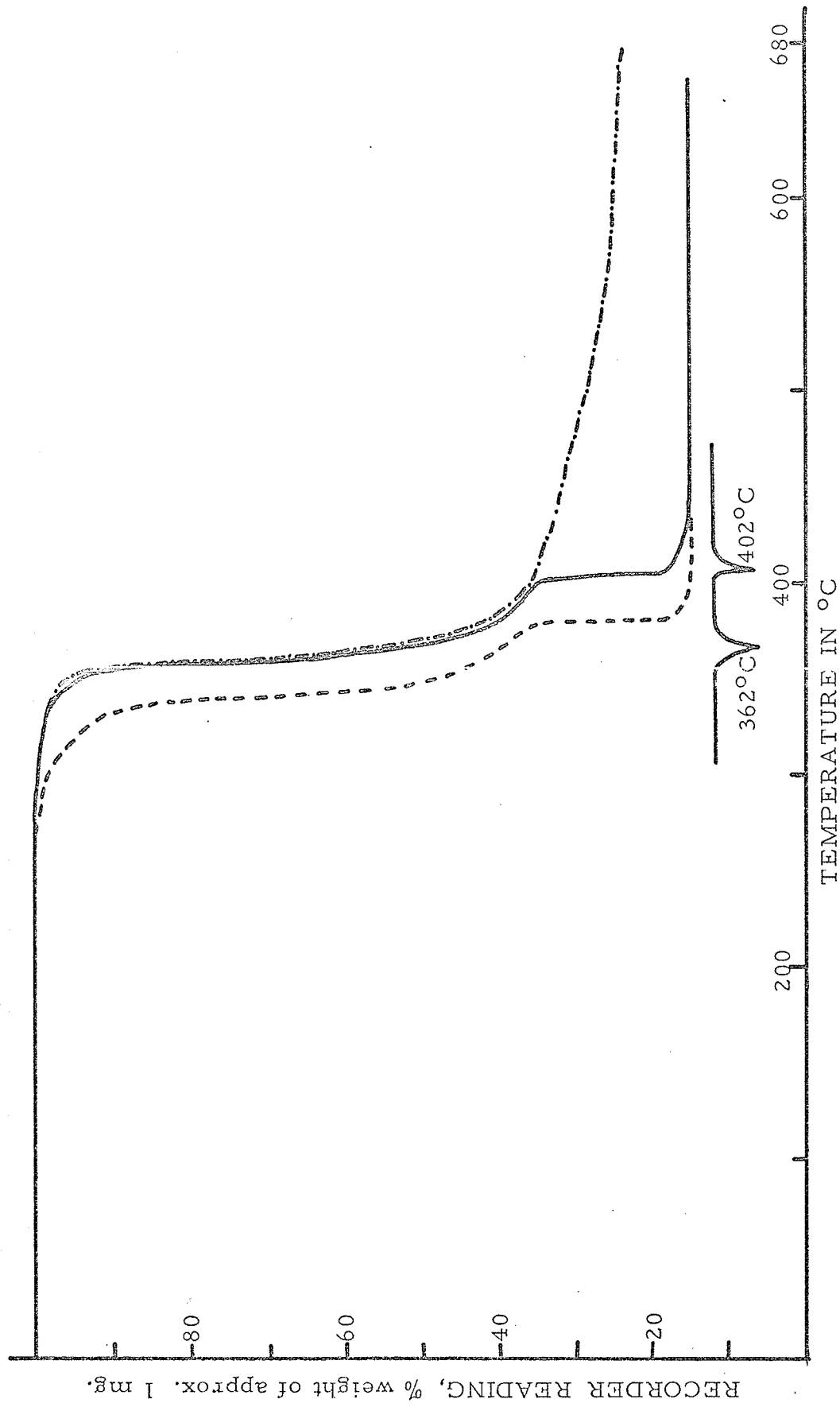


FIG. 14 THERMOGRAM. OF Ni(DPG)<sub>2</sub>

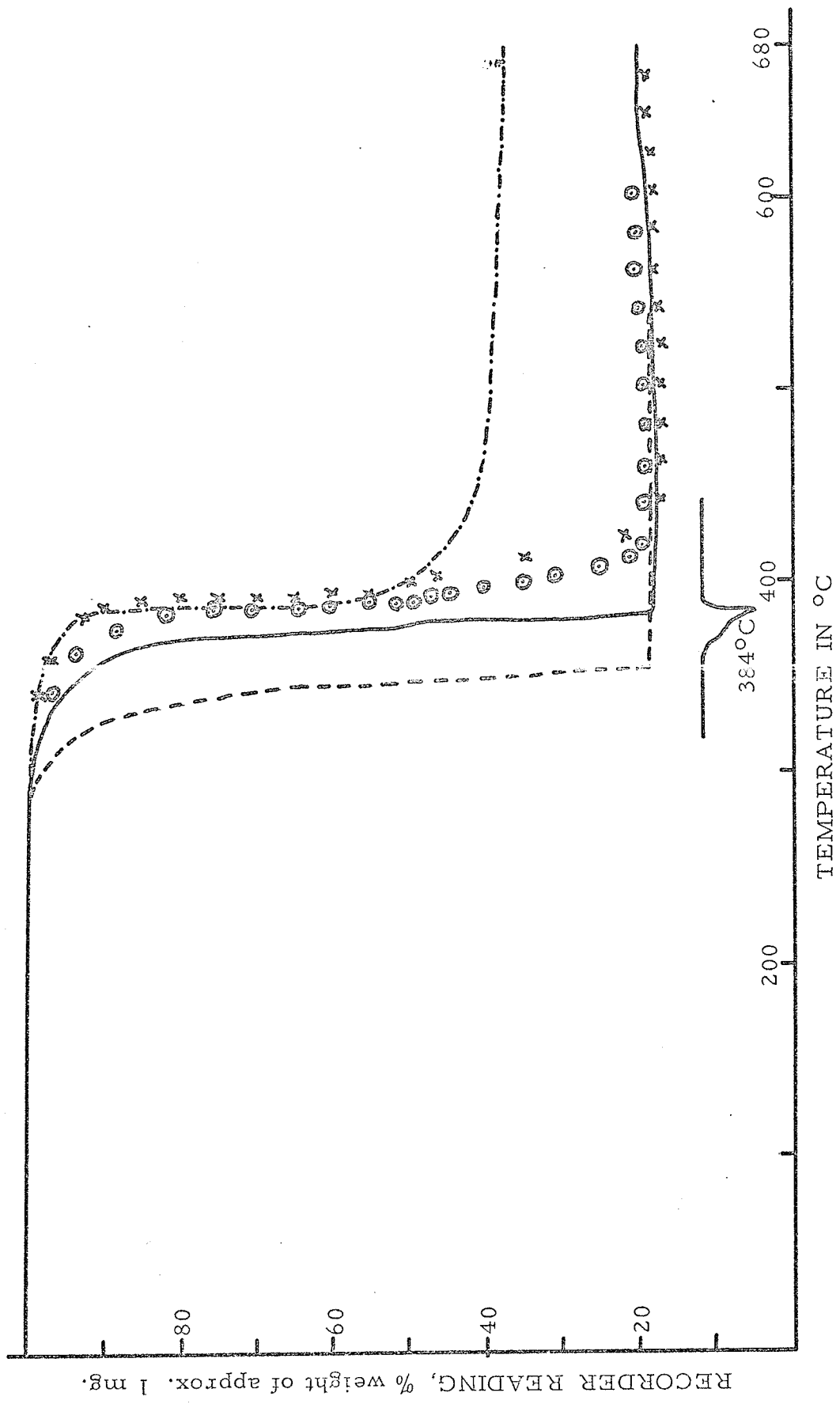
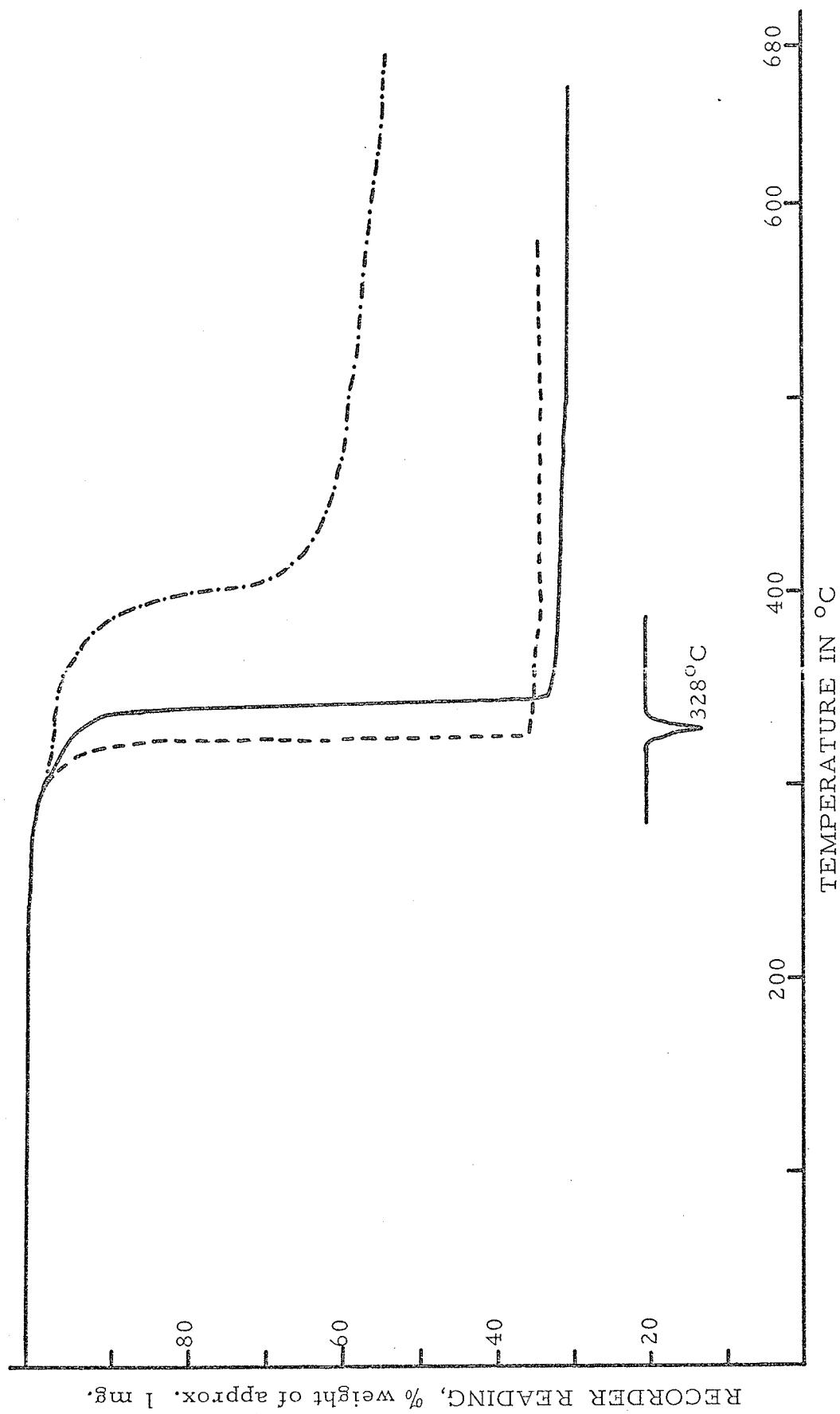
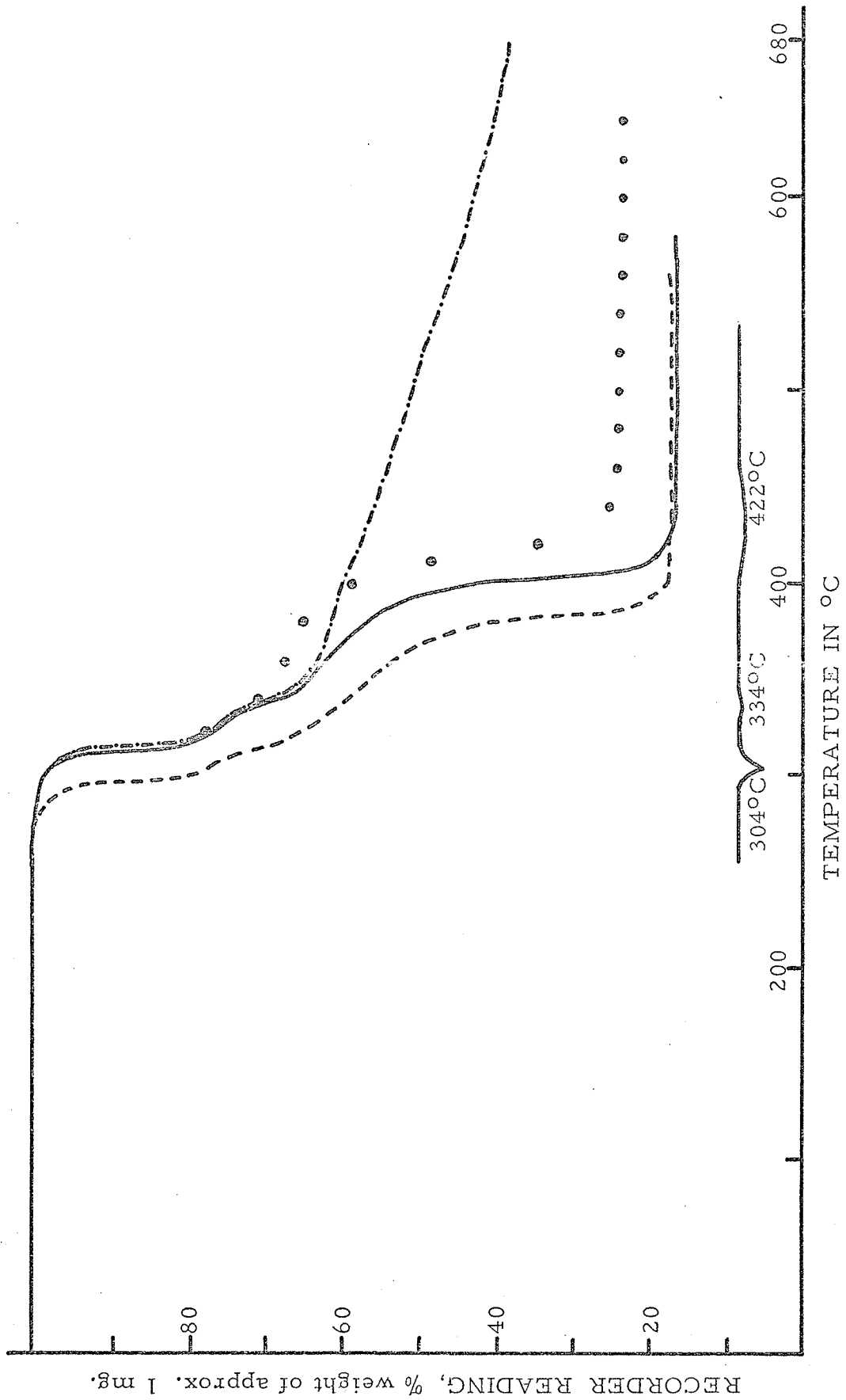


FIG. 15 THERMOGRAM OF Pd(DPG)<sub>2</sub>

FIG. 16 THERMOGRAM OF  $\text{Pt}(\text{DPG})_2$

FIG. 17 THERMOGRAM OF Ni( $\alpha$ -DFD)<sub>2</sub>

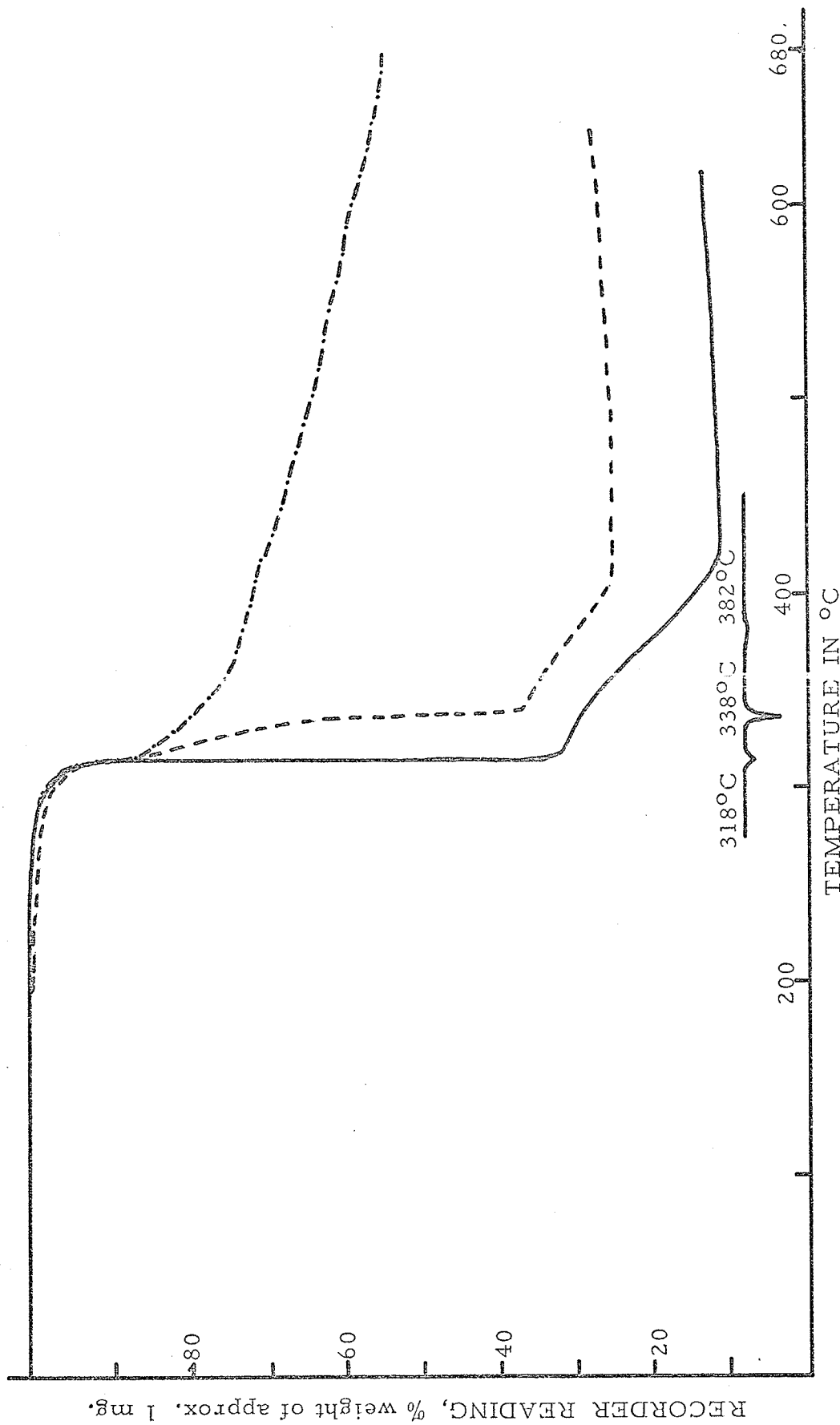


FIG. 18 THERMOGRAM OF Pd(ox-DFD)<sub>2</sub>

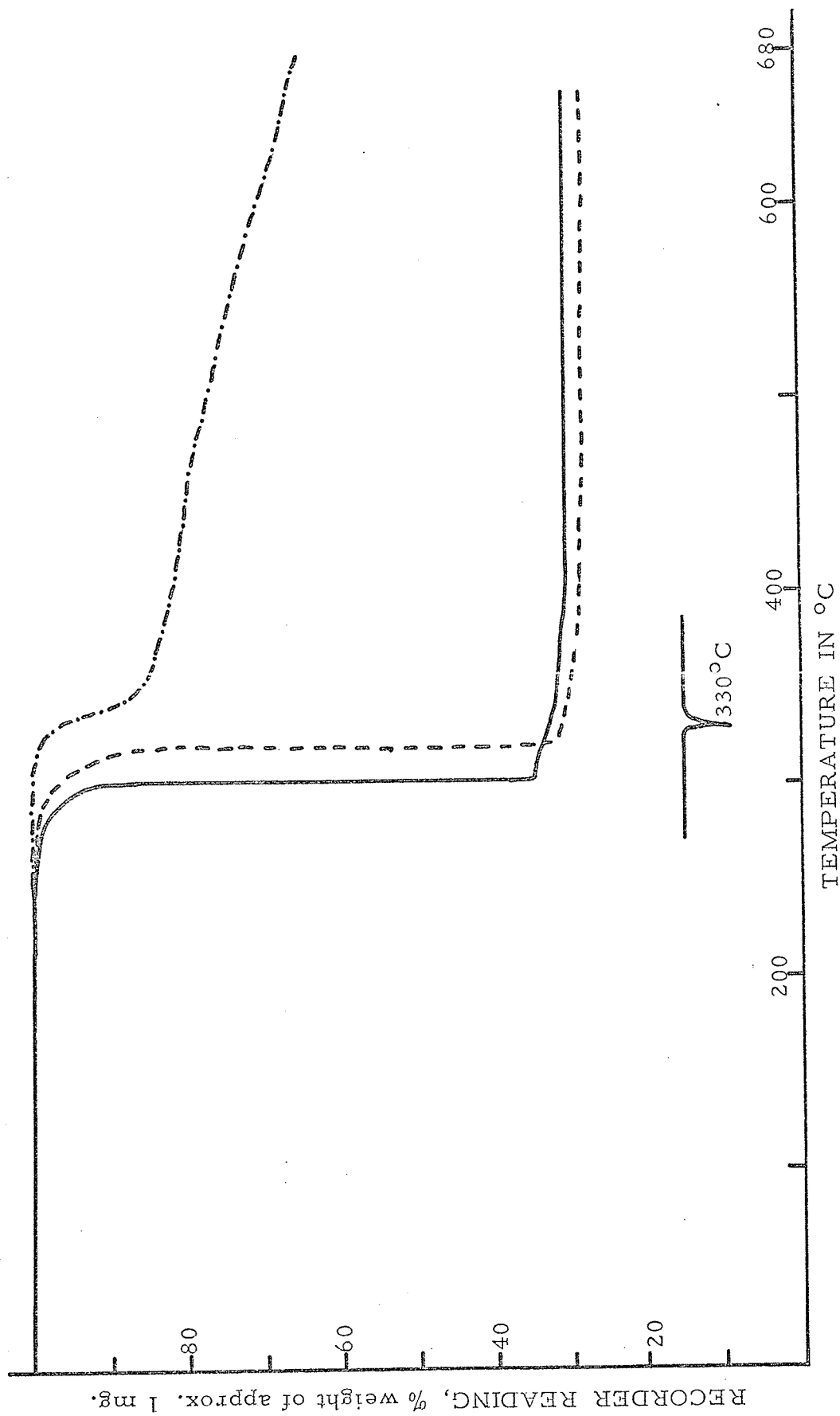
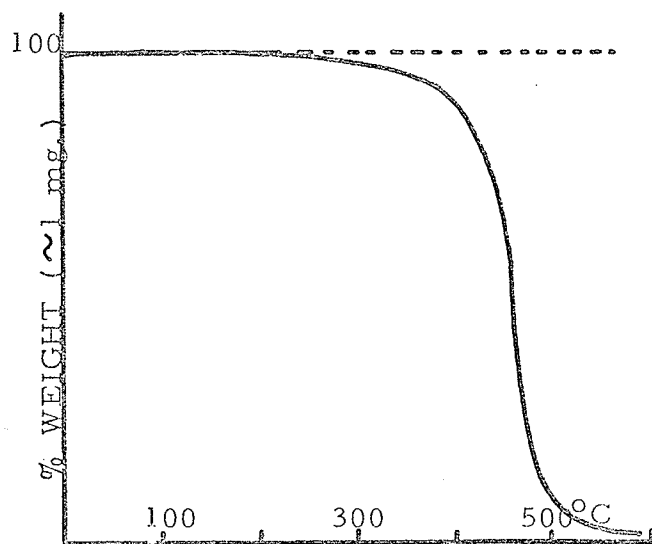
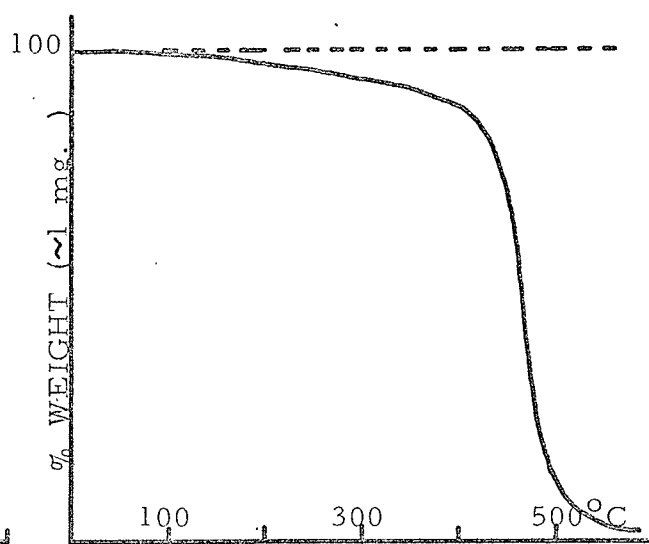
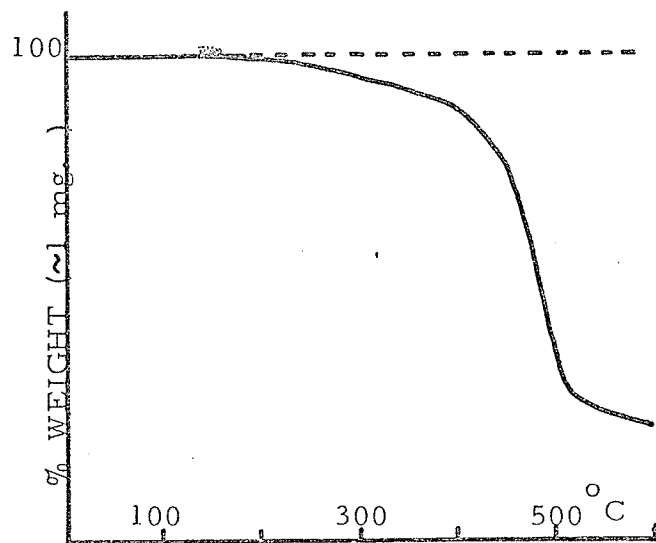


FIG. 19 THERMOGRAM. OF Pt( $\alpha$ -DFD)<sub>2</sub>

FIG. 20

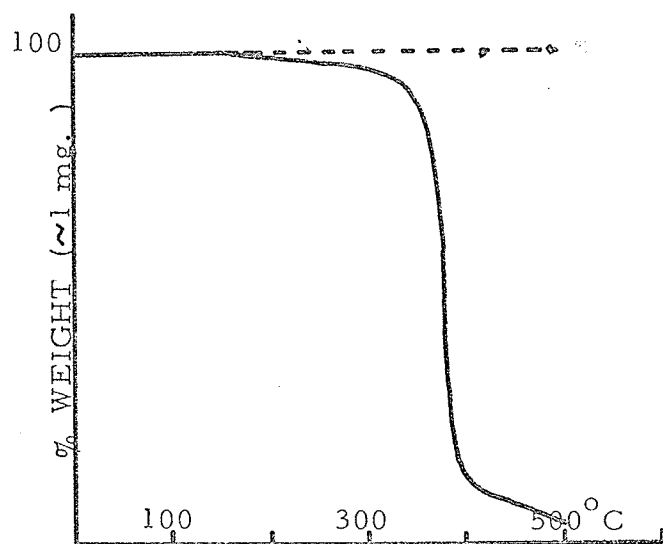
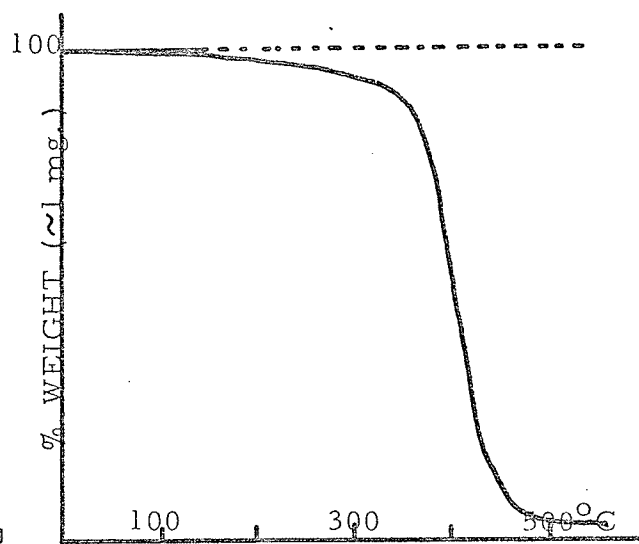
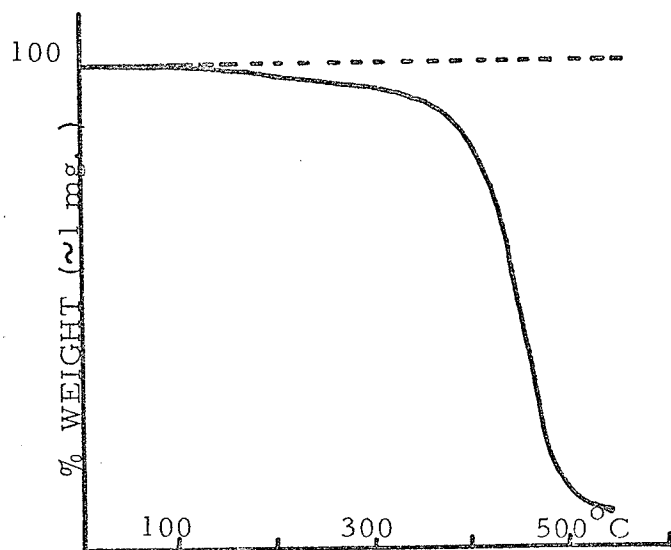
THERMOGRAMS OF METAL  
DIPHENYLGLYOXIMATES  
OBTAINED IN VACUUM

(a) Ni(DPG)<sub>2</sub>(b) Pd(DPG)<sub>2</sub>(c) Pt(DPG)<sub>2</sub>

ALL THREE RUNS  
AT 10°/MIN.

FIG. 21

THERMOGRAMS OF METAL  
 $\alpha$ -FURILDIOXIMATES  
OBTAINED IN VACUUM

(a) Ni( $\alpha$ -DFD)<sub>2</sub>(b) Pd( $\alpha$ -DFD)<sub>2</sub>(c) Pt( $\alpha$ -DFD)<sub>2</sub>

ALL THREE RUNS  
AT 10°/MIN.

of the sample at a rate which is faster than the heating rate of the furnace, accelerating the whole decomposition process. This could also be the explanation of the difference in our values of the decomposition temperature and those obtained by Duval. (32) (table V) He used sample weights of 250 - 300 mg. (36) compared to our small samples of 1 mg. Larger samples would definitely be subject to larger self-heating effects. At a lower heating rate, the temperature shift should be bigger, according to the above assumption, and this is clearly borne out to be the case. This temperature shift of the decomposition would depend on the amount of heat generated per mole and, of course, on other factors such as the form of the samples and how it is packed. In oxygen-free nitrogen, the thermograms are characterized by a sharp initial weight loss followed by a slow weight loss which is still continuing at the high temperature limit of the thermograms. We suggest that the initial weight loss is caused by decomposition of the complex with formation of some volatile decomposition products and some relatively non-volatile, high molecular weight organic compounds. During the subsequent slow weight loss, carbonization of these organic decomposition products occurs with release of volatile by-products. Table VI shows the colour of the residues left. In the cases of nickel and palladium diphenylglyoximates and  $\alpha$ -furyl-dioximates, a comparison of the thermograms obtained in oxygen and in nitrogen seems to show that oxygen catalyses or takes

part in the decomposition reaction at the later stage(s) only. The other thermograms do not show two well-defined steps in the weight loss stage due to overlapping reactions but we cannot exclude the probability that all decomposition reactions follow this pattern. It seems to be generally true from the slopes and decomposition temperatures of the thermograms that platinum complexes are thermally less stable than the nickel complexes.

No attempt has been made to correlate the above results with those obtained under vacuum, except for the shapes of the curves. The temperature calibration curve obtained under vacuum, with other parameters constant, is so different (by as much as  $89^{\circ}\text{C}$  in the extreme case when compared with manufacturer's values) that no significant comments can be made.

The remaining features of the thermograms will be discussed individually.

#### DIMETHYLGLYOXIMATES

Decomposition of the Ni(II), Pd(II) and Pt(II) dimethylglyoximates (or bis-(dimethylglyoximato)M(II) where M = Ni, Pd or Pt as these complexes are beginning to be called) occurs between  $330^{\circ}$  and  $355^{\circ}$  C. The thermograms for Ni(II) and Pt(II) appear smooth, but the decomposition is definitely not a first order reaction. They do not yield straight line graphs when the method of Horowitz and Metzger (36, 37) is applied. In this method, a plot of  $\log \log 1/x$  versus  $\theta$  is made, where  $x$  is the molar fraction of the initial

TABLE VI. RESIDUE CHARACTERISTICS OF VIC - DIOXIMATES  
AFTER HEATING IN AIR AND IN NITROGEN

COMPLEX		COLOUR		WEIGHT (Afterheating in air)			
		AIR	NITROGEN	%	wt. (a)	comment	(b)
DMG	Ni	grey	black	17.5	50	(c)	86
	Pd	br. -black	black	28.5-31	96-104	(c)	98
	Pt	grey	black	38	162	(c)	83
DPG	Ni	grey	grey	15.0	80	(d)	-
	Pd	br. grey	d. grey	17-19	105-117	(e)-(c)	-
	Pt	l. grey	black	30.0	202	(e)	-
<del>DL</del> -DFD	Ni	d. grey	d. grey	10.5	52	(c)	89
	Pd	br. grey	d. grey	11-13	64-67	(c)	56
	Pt	grey	black	30.0	190	(c)	97
Niox	Ni	d. grey	black	8.0	27	(c)	46
	Pd	br. grey	black	11.0	43	(c)	40
	Pt	d. grey	black	31.5	105	(c)	54
4MNIox	Ni	grey	black	19.0	37.5	(c)	64
	Pd	brown	grey-bk.	21-23	87-96	(c)	82
	Pt	grey	black	37.5	189	(c)	97

(a) - weight relative to 1 gm. molecular weight of starting material

(b) - (residue / atomic weight of metal) x 100

(c) - weight is less than metal

(d) - weight is heavier than the oxide, NiO, PdO or PtO<sub>2</sub>

(e) - weight is heavier than the metal but lighter than the oxide

complex remaining;  $\theta$  is the relative temperature according to the equation  $\theta = T - T_s$ ,  $T_s$  being the temperature when  $x = 1/e$  of the initial value. A downward break is observed for the Pd(II) complex at about 410°C (where it is most noticeable) and similar downward breaks are not observed in the other thermograms obtained in air, and this is in accord with Duval's results. (39) The downward break may be due to the onset of atmospheric oxidation. At the foot of the steep descents for Ni(DMG)<sub>2</sub> and Pt(DMG)<sub>2</sub> are regions where a further, slower and smaller weight loss occurs before the final plateau is reached. This region may be due to oxidation or volatilization of organic residues from the decomposition of the chelate.

For each metal chelate the weight of the final residue is less than that required for the formation of either the metal or the metal oxide. (Table VI) A reasonable assumption is that some sublimation of the chelate accompanies decomposition during the rapid weight loss stage or even during the earlier, slight gradual weight-loss stage. A red deposit in the case of Ni(DMG)<sub>2</sub> and a yellow deposit in the case of Pd(DMG)<sub>2</sub> (Pt(DMG)<sub>2</sub> is less discernible) were noted on the air cooled glass tube surrounding the furnace. This seems to contradict Duval's result on Ni(DMG)<sub>2</sub>. He denied the common belief of its sublimation (except in vacuo) but rather stated that "two NO groups are lost per molecule of the oxime." (39) However, two NO groups would constitute 10.4% of

the molecular weight and this is not very clearly shown on the thermogram. The gradual weight loss would be too slow for this reaction anyway. The diphenylglyoximates, as will be discussed later, give thermograms which have sharper curvatures and more abrupt decomposition stages and are the only series of compounds in this study which give residues heavier than either the metal or metal oxide (table VI). Also in trying to obtain mass spectra of them, we found that they are very sensitive to rise in temperature once the temperature high enough for the appearance of the parent peak is obtained. That is, they decompose very readily after that temperature. Thus we believe that sublimation is one of the steps that takes place in these compounds in the application of heat under an oxygenated atmosphere.

#### NIOXIMATES AND 4-METHYL-NIOXIMATES

Apart from qualitative differences the thermograms can be explained in much the same way as those of the dimethylglyoximates. The decomposition temperatures are rather lower than for the dimethylglyoximates, and the curves are steeper. Furthermore, it seems that for the nioximates a greater proportion of the weight loss is due to sublimation of the chelate than for the other complexes.

#### DIPHENYLGLYOXIMATES AND $\alpha$ -FURILDIOXIMATES

Except for the Pt(II) complexes, the thermograms are more complicated for these series of complexes than for the

previous ones. Three stages are apparent in the rapid descents in the thermograms of  $\text{Ni}(\alpha\text{-DFD})_2$  and  $\text{Pd}(\alpha\text{-DFD})_2$  and two stages in those for  $\text{Ni}(\text{DPG})_2$  and  $\text{Pd}(\text{DPG})_2$ . In each thermogram, one of these stages may characterize the advent of atmospheric oxidation and it would very likely be the last stage. This can be deduced from a comparison with thermograms obtained in dry nitrogen. Since the plateaux are not well-defined, it is not possible to assign a particular significance to any of the breaks in the thermograms with any confidence, particularly since the breaks do not occur at corresponding points in the thermograms, even on an atom per cent basis, but a common process is again not ruled out. The decomposition temperature of the  $\alpha$ -furildioximates are similar to those of the dimethylglyoximates, while those of the diphenylglyoximates are 20 - 30°C higher. As evidenced by the weights of the residues, less sublimation accompanies decomposition for the diphenyl- than for the  $\alpha$ -furyl- complexes.

Thus it appears that the decomposition of the DMG, Niox and 4MNiox complexes is fairly straightforward (although the nature of the volatile products may be complicated), while a detailed understanding of the thermograms of the other two series requires further study. The thermograms show that, under the conditions employed, little significant decomposition occurs below 250°C for any of the complexes. These conditions admittedly are very different from the background vacuum of the mass

spectrometer which is approximately  $1 \times 10^{-6}$  torr, yet since the sample temperatures required to obtain a mass spectrum were lower than the decomposition temperature by about  $100^{\circ}\text{C}$  in most cases, it seems likely that any thermal decomposition that occurs in the mass spectrometer probably occurs within the ion source itself (ambient temperature about  $250^{\circ}\text{C}$ ) rather than during heating the sample. And this result makes the interpretation of their mass spectra feasible.

CHAPTER THREE  
MASS SPECTRAL STUDIES

## SECTION I. INTRODUCTION

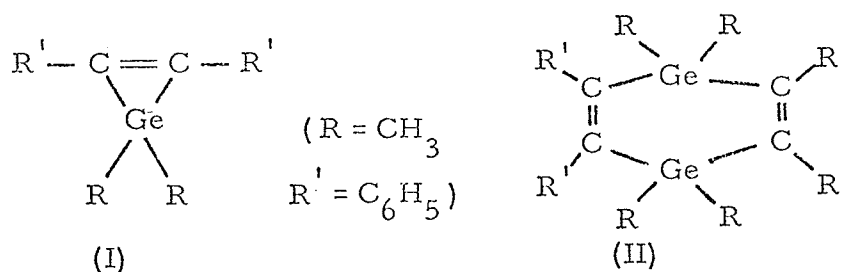
The beginning of the mass spectrometry era dated back to as early as 1886 when Goldstein discovered the so-called 'canal rays'. (40) J. J. Thomson (41) then invented an apparatus to separate these rays according to their mass to charge ratio and this is the first mass spectrometer of its kind man had ever made. Later, Aston (42), Dempster (43), Cameron and Eggers (44), Craig (45), Nier (46), Mattauch and Herzog (47) and others improved his instrument by devising various types of mass spectrometers with much more sophisticated inlet systems, ion sources, deflection and ion discrimination techniques, ion optics and detection devices to give instruments of higher resolution and better sensitivity.

Since then, the field of mass spectrometry has been vastly expanded and theories (such as the quasi-equilibrium theory (48) and related rate constants (49, 50) and appearance potential determinations (51)) and proposed mechanisms for basic steps of decomposition of molecules (such as the McLafferty Rearrangement and odd- and even-electron ion relationship (52)) were written by people related to this branch of science.

The instrument has been engaged in structure determination under various conditions such as energy of bombarding electrons and temperature of samples. It can also be used in free radical studies, radioisotopic half-life, isotopic abundance and precise atomic weight determinations. Detection of ions formed in a

chemical reaction (chemi-ionization process) can be achieved by means of a mass spectrometer. In the more adventurous nowadays, a mass spectrometer can also find itself being used in upper atmosphere research. Man has been able to obtain valuable information about the space (e. g. exosphere or ionsphere) using a quadrupole, time-of-flight or radiofrequency mass spectrometer installed in a rocket or satellite depending on the objective of the experiment. (53)

The use of mass spectrometry in the study of inorganic compounds, both qualitatively and quantitatively (54, 55, 56, 57, 58) has become more and more important. By the use of it, structure and molecular weight determination in most cases become easier. For example, the germanium complex  $\text{Ge}(\text{C}_2\text{R}_2)\text{R}_2$  was confirmed to be a dimer (II) rather than a monomer (I) only through the use



of a mass spectrometer. (59) From fragmentation patterns and appearance potentials, certain chemical properties such as chemical bonding (with  $\sigma$  or  $\pi$  orbitals), molecular and electronic structures and mechanisms of decomposition can sometimes be deduced.

The mass spectra of transition metal vic-dioximates have not been reported to date except those given by Jenkins

Majer (60) for Ni(DMG)<sub>2</sub> and Ni(DPG)<sub>2</sub>. However, their interest lay mostly on the quantitative point of view and no explanation of the fragmentation of these compounds was attempted.

It has been discussed earlier that in the vic-dioximates electrons are very likely partially delocalized around the chelate ring, though not as effectively as in the acetylacetonates (61) which can even undergo aromatic type substitution on the ring. A study of the fragmentation patterns of the dioximates with different substituent groups may lead to an improved understanding of these compounds. A comparative study between the TGA results and those obtained from mass spectrometry can also be made.

## SECTION II. INSTRUMENTAL - THE HITACHI RMU - 6D MODEL

Most mass spectrometers will be found to consist of the following, (i) the inlet system, (ii) the ion source, (iii) the electrostatic accelerating system and mass analyser and (iv) the ion collector, amplifier and read-out system.

The inlet system for the Hitachi RMU-6D model used in this work is as follows; Solid is admitted through a direct insertion probe. Gas (through the gas line reservoir system) or liquid (whose heated vapour goes in by way of the gas reservoir) are admitted through a pin hole into the ionization chamber.

The ion source employs the electron bombardment technique and is the heart of the mass spectrometer. It consists

mainly of an ionization chamber, a pair of repellers, a pair of lens electrodes, a grounded electrode, a filament, a target, a sample block-heater right by the side of the insertion probe and thermocouples for measuring temperatures. Cross-sectional views of the ion source can be seen from fig. 22.

The filament is the source of electron supply and the electron current emitted is kept constant (filament current is 3-3.5 amps. and its temperature is about  $1700^{\circ}\text{C}$ ) by the emission regulator supplied by a stabilized voltage. Rhenium wire is preferred as the filament material over the more readily obtainable tungsten wire simply because of its better ductility at all temperatures and is thus less likely to be ruptured by thermal or mechanical work and because of the fact that it is easily spot welded, is more resistant to the attack of water formed from various decompositions, forms unstable carbides, is not gas-sensitive and its melting point and thermal work function are only slightly below those of tungsten (62).

The electrons emitted are accelerated to 50-70 volts and enter the ionization chamber. The diverging angle of the electron beam is minimized by the use of a grid electrode in the filament assembly and a collimator magnet outside the ion source assembly. The magnetic field is a weak 100-200 gauss field but it certainly prevents contamination (from deposition of electrons onto the walls before going into the ionization chamber) and ensures

a greater probability of ionization of sample molecules (by giving more electrons for collision).

The electrons, after passing through the ionization chamber, are caught by the target electrode. A maximized target current is obtained by adjusting the collimating electrodes and repeller voltage so as to give the electron optical system its best working conditions.

Some of the electrons, on their way from the filament to the target collide with the gaseous sample molecules, which came in through the orifice, and ionize the latter. These ionized molecules are pushed out towards the ion accelerating field by a potential gradient established between a pair of repellers and a pull slit of the chamber. Between the pull slit and the ground electrode, a stabilized D. C. high voltage is applied which is able to accelerate the ions. The maximum acceleration is 3600 volts; stepwise down to 2400, 1800, 1200, 900, 600 volts. The stabilized D. C. high voltage is rectified and smoothed from a high voltage of A. C. 5000 volts.

By adjusting the voltages of two lens electrodes, situated in between the two accelerating electrodes, the ions formed can be focussed and ejected as a beam of narrow aperture through the exit slit into the analyzer tube. Here the ions are deflected in traversing (fig. 23) by influence of a homogeneous magnetic field at right angles to the ion beam path. They then fall on the collector

FIG. 22

CROSS-SECTIONAL VIEW OF ION  
SOURCE OF HITACHI RMU-6D  
MASS SPECTROMETER

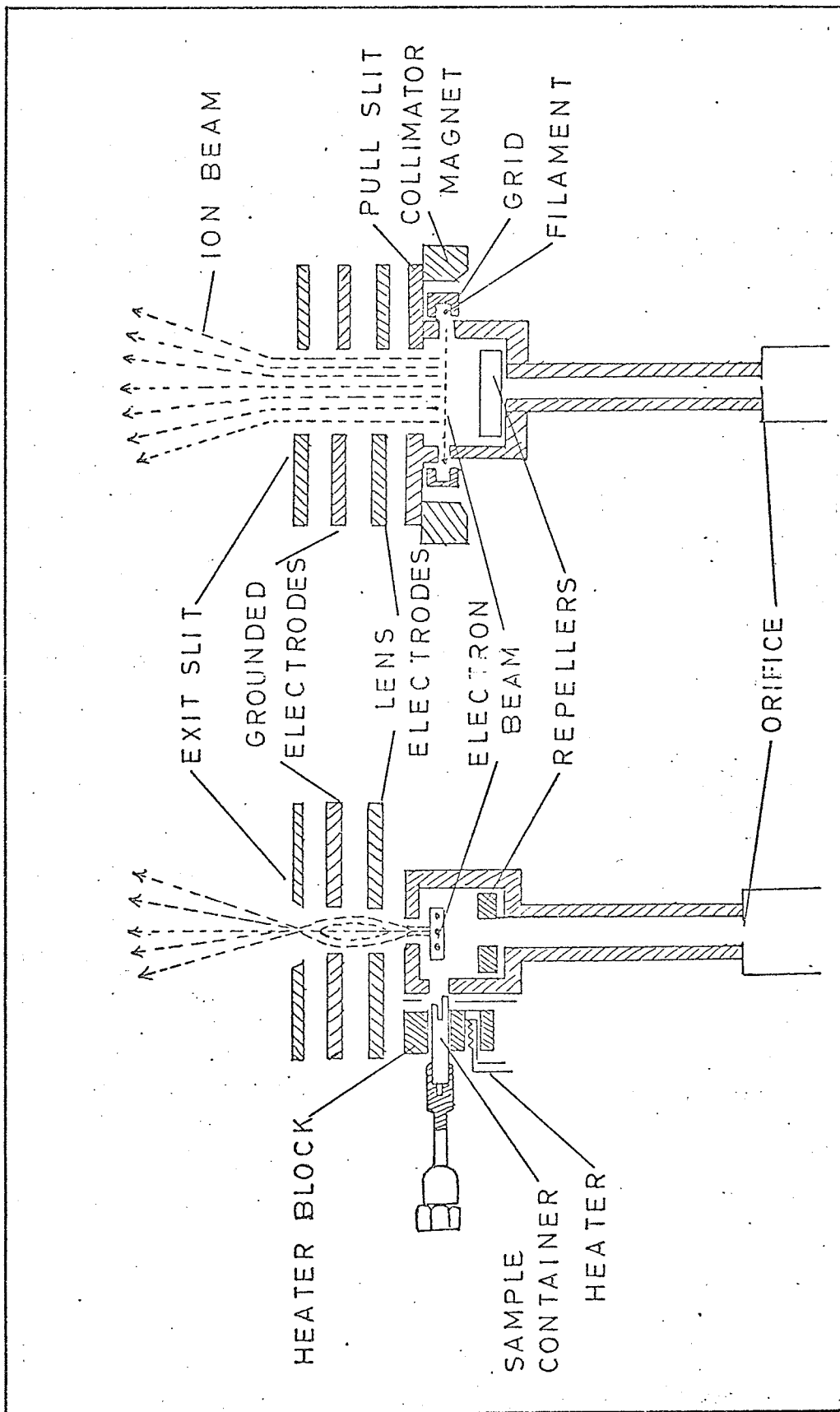


FIG. 23

MASS DISPERSION IN  
THE MAGNETIC FIELD

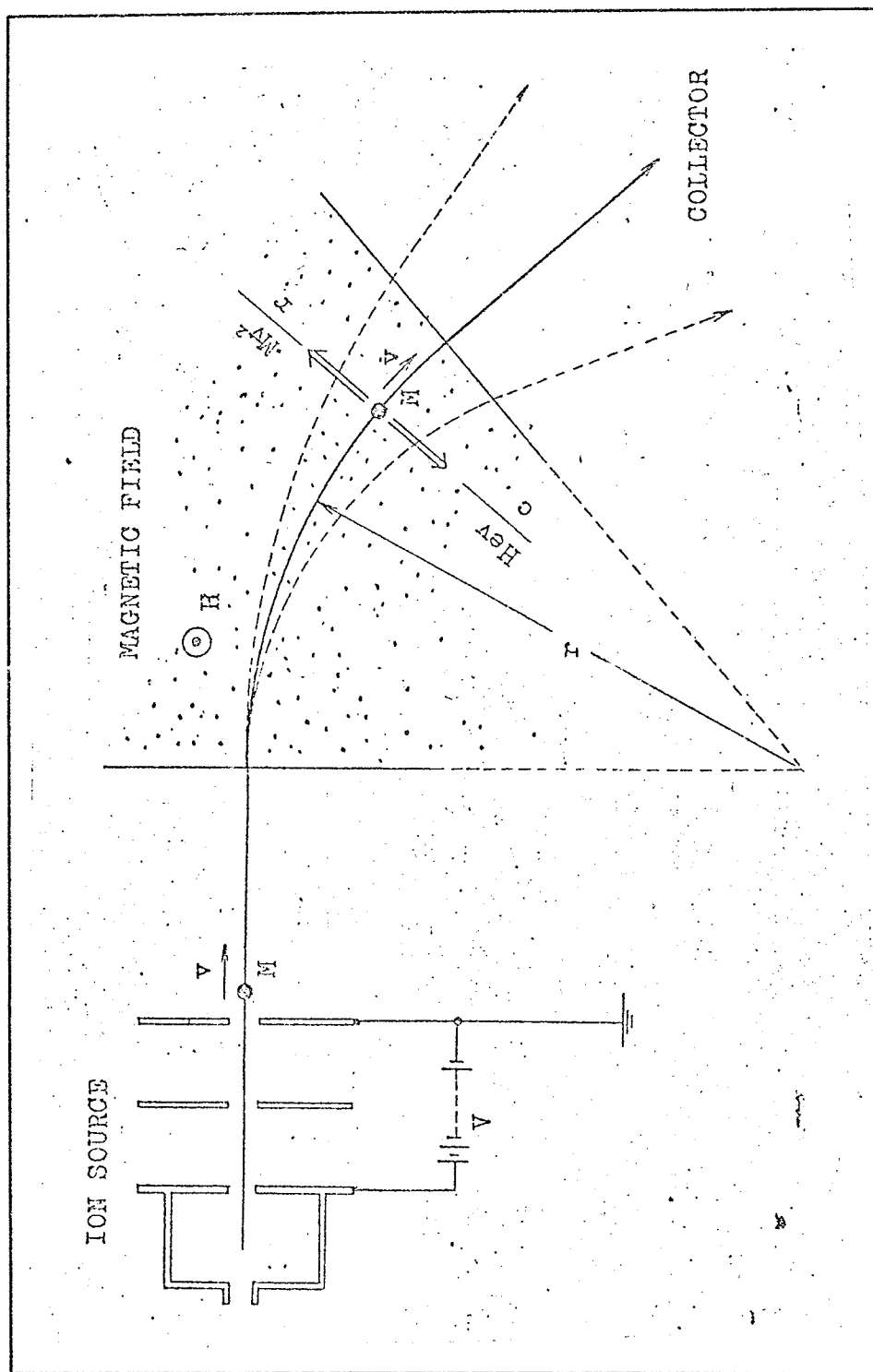
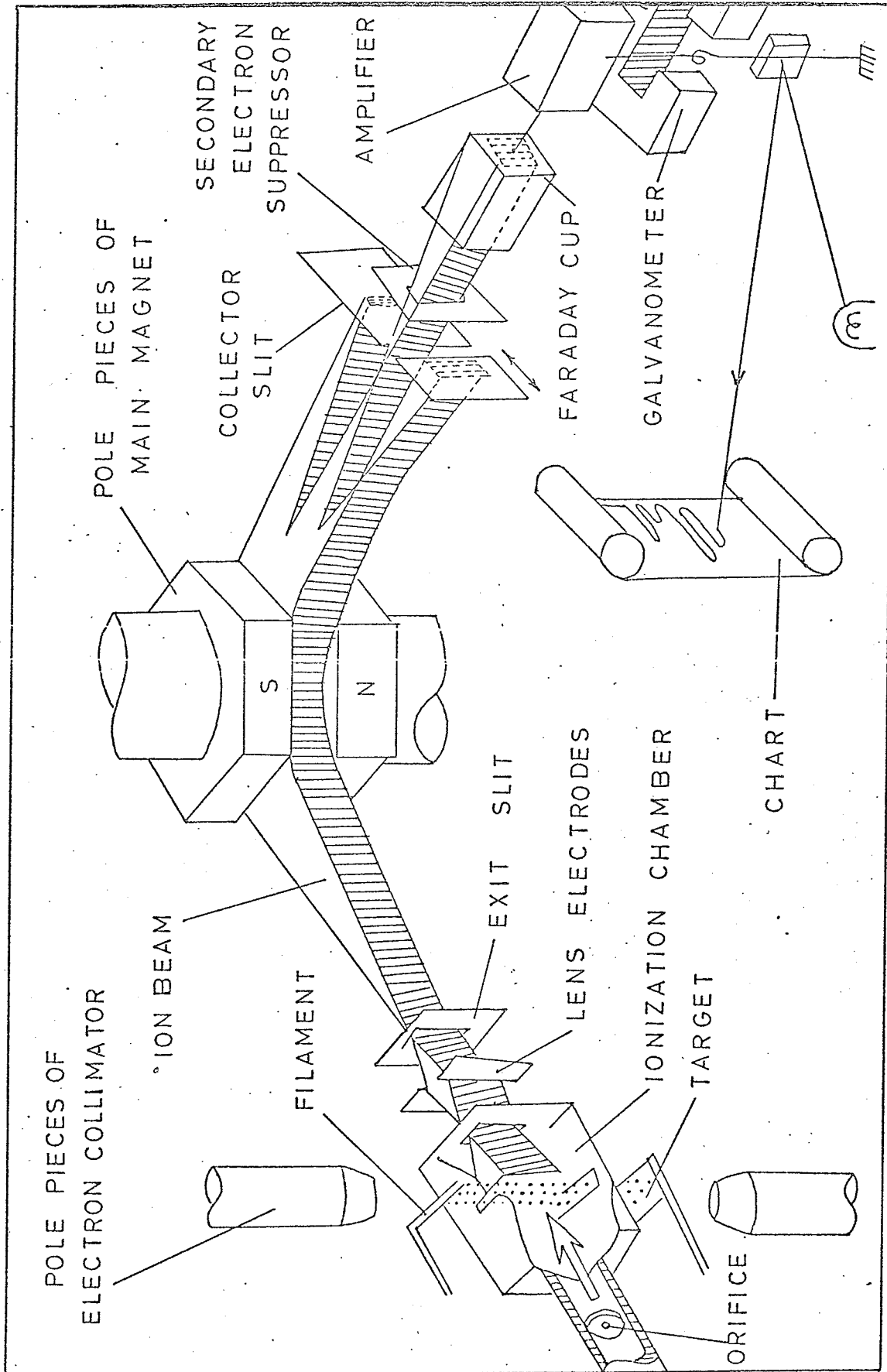


plate and amplified and recorded as a mass spectrum. A general layout of the mass spectrometer is shown in Fig. 24.

It might be appropriate to say here something more about ionization of the gaseous molecules. The ionization in the ionization chamber is carried out in the instance described above, and in the machine used here, by electron bombardment by electrons emitted from the filament. Other ionization procedures include photoionization, gaseous or arc discharge or hot spark source. These are not used as often. These electrons, as mentioned before, are usually accelerated through a voltage of 50-70 volts, and as the first ionization potential of most molecules or atoms seldom exceed 15 electron volts, there will be surplus energy. This extra energy will either be dissipated away as kinetic energy, or most likely some will be absorbed into the vibrational modes of the molecules. This may result in unimolecular dissociation, and the formation of various kinds of ions, and neutral fragments. These ions form a mass spectrum, or pattern coefficient, of a compound. The transition of energy is assumed to be radiationless and to follow closely the Franck-Condon Principle. (63, 64) The theoretical prediction of a mass spectrum presently employs a statistical theory called the quasi-equilibrium theory, which assumes that the excited molecular ion does not decompose immediately after impact into the various fragment ions and neutral species but rather there is a time lag

FIG. 24

LAY-OUT OF ION SOURCE,  
ANALYZER AND DETECTOR OF  
RMU - 6D MASS SPECTROMETER



when it would undergo several vibrational transitions and then would decompose only after sufficient energy has been accumulated in the necessary degrees of freedom of the molecular ion. The energy transfer into the molecular ion upon ionizing collision can be described by the Maxwell-Boltzmann energy distribution relationship and this transferred energy together with the internal energy distribution are carried over into the various vibronic levels according to the Franck-Condon Principle. The molecular ion then decomposes through different competing steps whose rate constants can be calculated on the basis of the equilibrium between the reactant and activated complexes. Information about these rate constants will enable the theoretical calculation of the intensities of peaks obtained as a result of these decompositions. However there are still two major regions that have not been clarified and they are still a matter of theoretical interest. First, the kinetics between the reactant and activated complexes in an isolated system such as one inside the ion source is still unexplored and expressions used to calculate rate constants need to be modified if better results are to be expected. Secondly, the transition of the excitation energy (sum of distribution of energy transfer and distribution of internal energy) may not be transformed into the vibrational energy levels through a Maxwell-Boltzmann distribution, so that the internal energy is not conserved as a result of the Franck-Condon transitions. A Gaussian distribution has been used in some cases, especially in

metastable transitions.

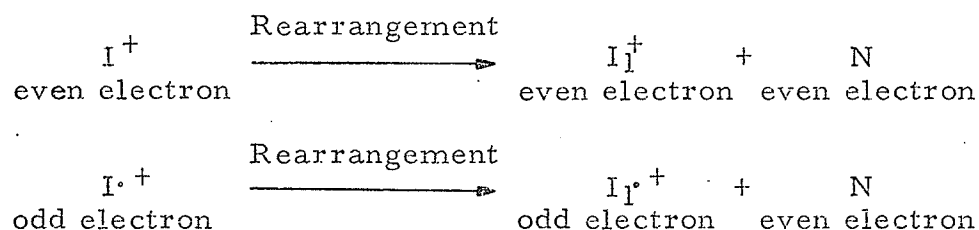
The various types of ions formed as a result of dissociation of the molecule are described as follows. (65)

The parent ion is the ionized sample molecule (molecular ion), or the ion which gives out fragment ions. In most cases, they will be singly charged. However, since the second ionization potential of most molecules is only several electron volts above the first ionization potential ( $IP(I) + IP(II) < 30 \text{ ev}$ ), the 50 volt electron impact can remove more than one electron easily and for some compounds there are many parent ions that are doubly- or multiply-charged.

Negative ions are produced through (1) electron capture, or (2) ion-pair production. The number of them produced in ordinary mass spectral conditions is small and they are of much smaller ion intensities. There has not been much attention paid to them yet, and little is known about negative ion mass spectrometry of organometallic compounds. (66)

Rearrangement ions are produced by rearrangement of atoms during unimolecular decomposition of the parent ion (molecular or fragment ion). They are stable fragment ions and are formed whenever energetically favorable. Rearrangement of an ion can be either "specific" or "random" depending on whether or not the process follows a well-defined path due to the presence of certain structural features. In a rearrangement process, an even electron

neutral molecule is eliminated so that if  $I^+$  represents an ion, and N a neutral molecule, then the following relationship holds for organic compounds, and organometallic or inorganic compounds where there is no accompanying change in valence state of the metal :



In cases where a change of metal valence state of one during fragmentation prevails, for example, an odd electron ion will give a formally even electron ion. Rearrangements are very common and frequently involve hydrogen and fluorine, although migration of other groups such as phenyl has been observed. Examples of fluorine compounds which have been studied are fluorinated acetylacetonates (61) and examples of hydrocarbons (unsaturated or saturated branched chain) can be found easily. (65, 66)

The energy obtained by the sample molecules as a result of electron impact will cause decomposition. However, some decomposition reactions are slow, of the order of 1  $\mu$ sec., while the path time from the ionization chamber to collector is about  $10^{-6}$  to  $10^{-7}$  sec. Thus these parent ions (each of mass  $m_0$ , decomposing finally into some neutral fragment(s) and another positive ion  $m_1$ ) will

"carry over" their decomposition out of the potential field into the analyser tube as metastable ions. Their path, in terms of the parent ion and daughter ion if they decompose in the accelerating field  $V_1$ , is described by (67)

$$r = \left( \frac{2V}{H^2 e} \right)^{1/2} \frac{m_1}{m_0} \left[ 1 + \frac{(m_0 - m_1)(V - V_1)}{m_1 V} \right]^{1/2} \quad (1)$$

However this is also the radius of curvature that an ion of mass  $m^*$  would travel through the magnetic field  $H$  travelling with a velocity accelerated by a potential  $V$ , i. e.

$$r = \left( \frac{2V}{H^2 e} \right)^{1/2} (m^*)^{1/2} \quad (2)$$

Thus an important relationship is obtained first derived by Hipple, Fox and Condon (68):

$$m^* = \frac{m_1^2}{m_0} \left[ 1 + \frac{(m_0 - m_1)(V - V_1)}{m_1 V} \right] \quad (3)$$

where  $m^*$  = apparent mass of the metastable ion

$m_1$  = mass of the daughter ion

$m_0$  = mass of the parent ion

$V$  = full accelerating potential

$V_1$  = potential at certain point of the accelerating potential

field at which the decomposition of the metastable

ion occurs

However, metastable ions formed at large values of  $(V - V_1)$ , i. e. near the ion source, will not be detected because of their short lifetime (1 psec) and also the decomposition would sometimes release internal energy with the result that fragments formed will fly in all directions without having a good chance to go through the slit to the collector plate. Thus metastable ions detected are usually those formed at low values of  $V - V_1$  and a simplified equation is obtained:

$$m^* = \frac{m_1^2}{m_0} \quad (4)$$

They usually occur at much lower intensities (0.01 - 0.1% of the base peak) (65) and are diffuse and appear at non-integral masses (which can be deduced from equations (3) and (4)). Their intensity varies linearly with pressure of the original sample, and they depend on exit slit width and ion repeller electrodes just as other ion peaks do.

Metastable ions are, in fact, products of metastable transitions. They arise by the same mechanism as ordinary ions except for the time delay in the dissociation of the parent ion. Whether each metastable ion goes through two (Hipple's original study) or three (Coggeshall (69) and Momigny (70)) transition steps before dissociating to a positive ion and other neutral fragments is still an open question, but it has been concluded that there is a continuous

distribution of rate constants for the reaction (71, 72). Since each of these peaks corresponds to the formation of an ion of a particular structure and also to the breaking up of an ion of this empirical formula, their presence provides valuable clues to the identification of ions. The appearance potential of an ion resulting from a metastable ion would be the same as one resulting from an ordinary dissociation process; their values can be compared to confirm the assignment.

It has been found that double-ionization is the result of a simple electron impact process since the residence time of the parent ion in the ionization chamber is too short to permit the bombardment of a second electron. (73) The abundance of doubly-charged ions (the easiest type of multiply-charged ions to obtain) is usually low (74) and their relative intensities are usually small compared with those of singly-charged ions. The first example to have (1969) in which a doubly-charged ion has a relative intensity greater than singly-charged ions has been reported by Solomon and Mandelbaum: 4b, 9b-dibromo-4b, 5, 9b, 10-tetrahydroindeno(2, 1-a)inden-5, 10-dione. (75) They attributed this phenomenon to their relative stabilities, i. e. the exceptional stability of the doubly-charged ion and the relative instability of the singly-charged ion. Indeed, it is a necessary condition for multiply-charged ions to appear and they are most usually observed in aromatic or hetero-aromatic compounds or molecules which do not contain bonds which can undergo rupture

easily.

### SECTION III. EXPERIMENTAL - MASS SPECTROMETER OPERATION CONDITIONS AND IDENTIFI- CATION OF MASS SPECTRA

All the samples used here were the same as those used in the TGA studies. Any complexes that were reprepared were checked by their mass spectra with the ones obtained from samples used in the thermoanalysis experiment.

Deuteriation of  $\text{Ni}(\text{DMG})_2$  at the oxygen atoms was found to be difficult following the method described by Godycki, Rundle, Voter and Banks. (76) 50% deuteriation was achieved by dissolving the complex in dimethylsulfoxide (DMSO) and refluxing the solution with deuterium oxide for about an hour at  $50^\circ\text{C}$ .

The Hitachi Perkin-Elmer RMU - 6D single focussing mass spectrometer equipped with a T - 2M ion source was used to obtain all the mass spectra. For each run, the following conditions were satisfied:

Filament Current	= 3 amps.
Accelerating Voltage	= 1200 volts.
Chamber Temperature	= $220 - 250^\circ\text{C}$ .
Electron Energy	= 50 volts.

The spectra were recorded on a Honeywell-1508 visicorder. In recording a mass spectrum, reference is made to the highest

intensity metal-containing peak as the base peak in all cases. For very high masses, calibration of the mass scale was made with the help of perfluorokerosene (PFK).

Identifications of some of the peaks were made by use of the program written (table VII) using an IBM 360 computer. Various combinations of a peak value were obtained and unreasonable results were discarded. The deuteriated Ni(DMG)<sub>2</sub> complex also helped in the process of identification.

#### SECTION IV. RESULTS AND DISCUSSIONS

The mass spectra of the complexes formed between dimethylglyoxime, diphenylglyoxime,  $\alpha$ -furildioxime, nioxime and 4-methyl-nioxime with Ni(II), Pd(II) and Pt(II) are shown in figures 25 - 29. There are many peaks in the spectra, especially at low values of m/e. Those of Ni(DMG)<sub>2</sub> and Ni(DPG)<sub>2</sub> are similar to the ones given by Jenkins and Majer (60), except for one difference. Some of their nickel-containing peaks in Ni(DMG)<sub>2</sub> are one m/e unit less than ours. (Fig. 30) For example, some of their relatively intense peaks are 115, 173, 203 while our equivalent ones are 116, 174, 204. Comparison of these peaks with the spectrum of deuteriated Ni(DMG)<sub>2</sub> at the two hydrogens ( on the hydroxyl groups ) and with the spectra of the corresponding palladium and platinum complexes indicates that our assignments are more reliable.

As can be seen from tables VIII- XII each series of the

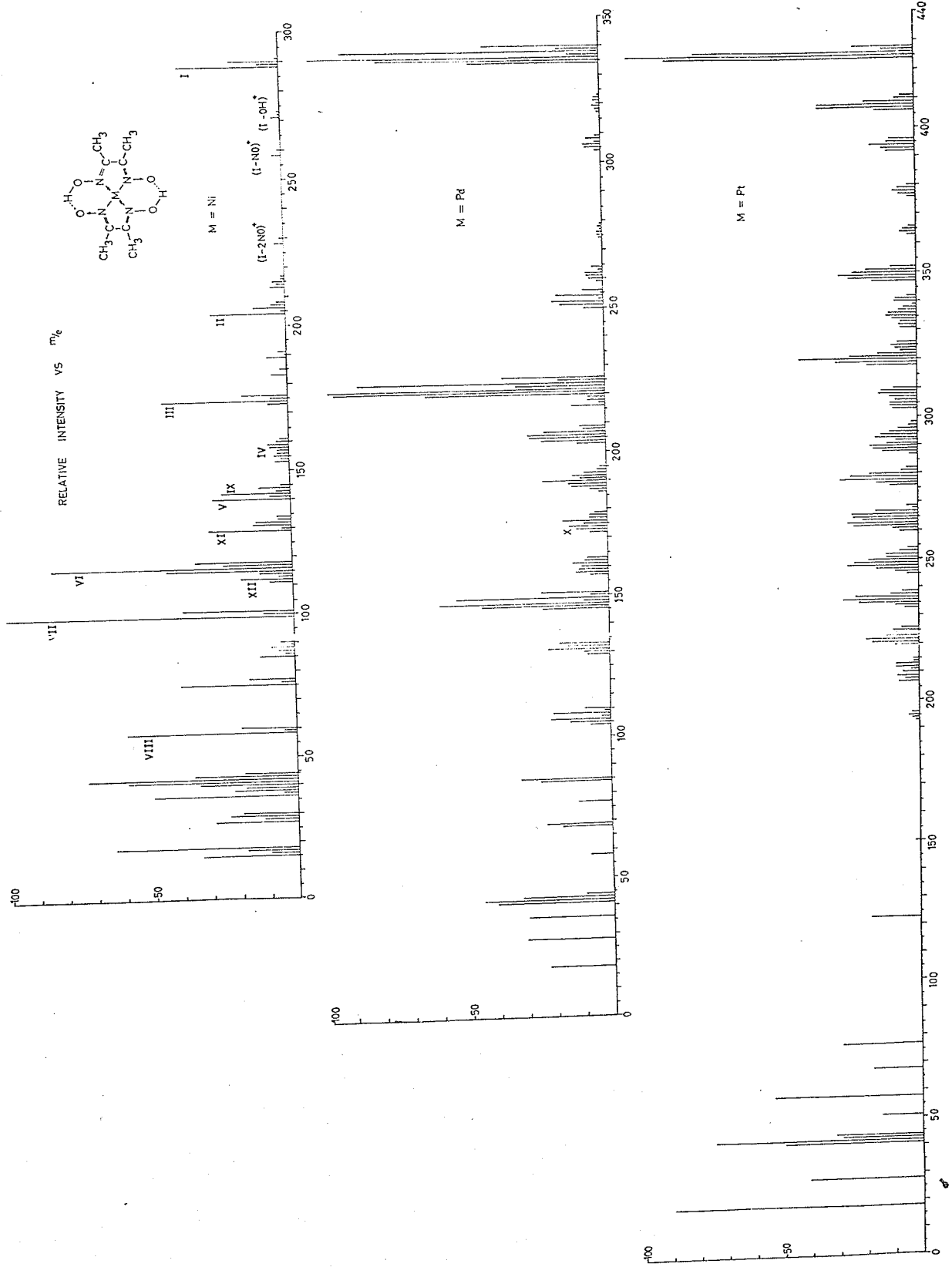
TABLE VII. IBM 360 COMPUTER PROGRAM FOR  
MATCHING PEAKS WITH ATOMS

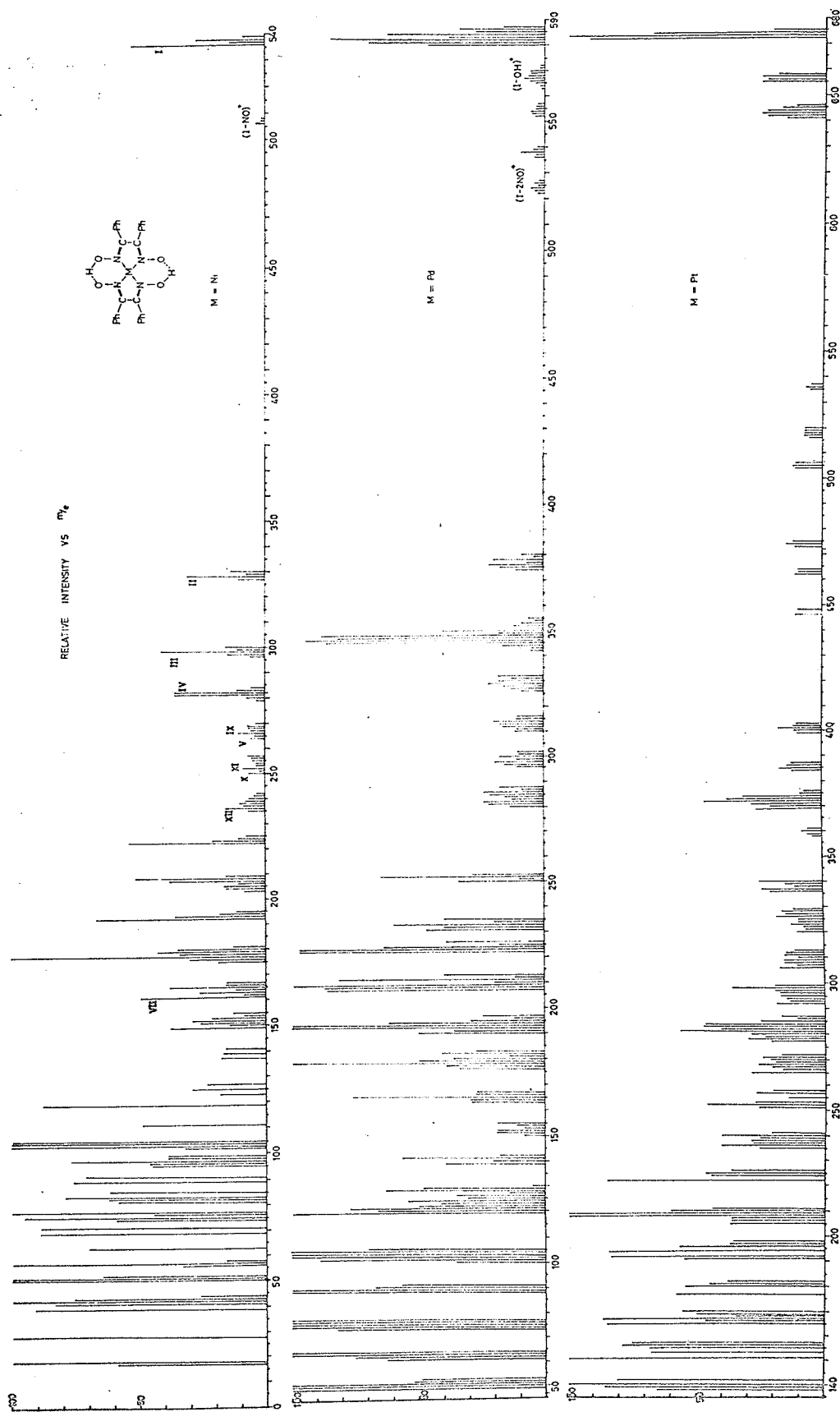
```
C      VALUES FOR DIMETHYLGLYOXIME
C      MATCHING PEAKS WITH ATOMS
C      I=Pt, 195, J=N2, 14, K=O2, 16, L=C, 12, M=H2, 1
      DIMENSION JCX(200)
      1 READ (5,100) (JCX(IJ),IJ=1,8)
100  FORMAT (8I10)
      DO 12 JI=1,8
      JC=JCX(JI)
      DO 12 IJ=.1,1
101  FORMAT (6I8)
      DO 12 I=0,1
      DO 12 J=0,4
      DO 12 K=0,4
      DO 12 L=0,28
      DO 12 M=0,22
      JX=I*195+J*14+K*16+L*12+M*1
      IF (JX.GT.JC) GO TO 12
      IF (JX.EQ.JC) WRITE (6,101) JC,I,J,K,L,M
      12 CONTINUE
      GO TO 1
999  CALL EXIT
      STOP
      END
```

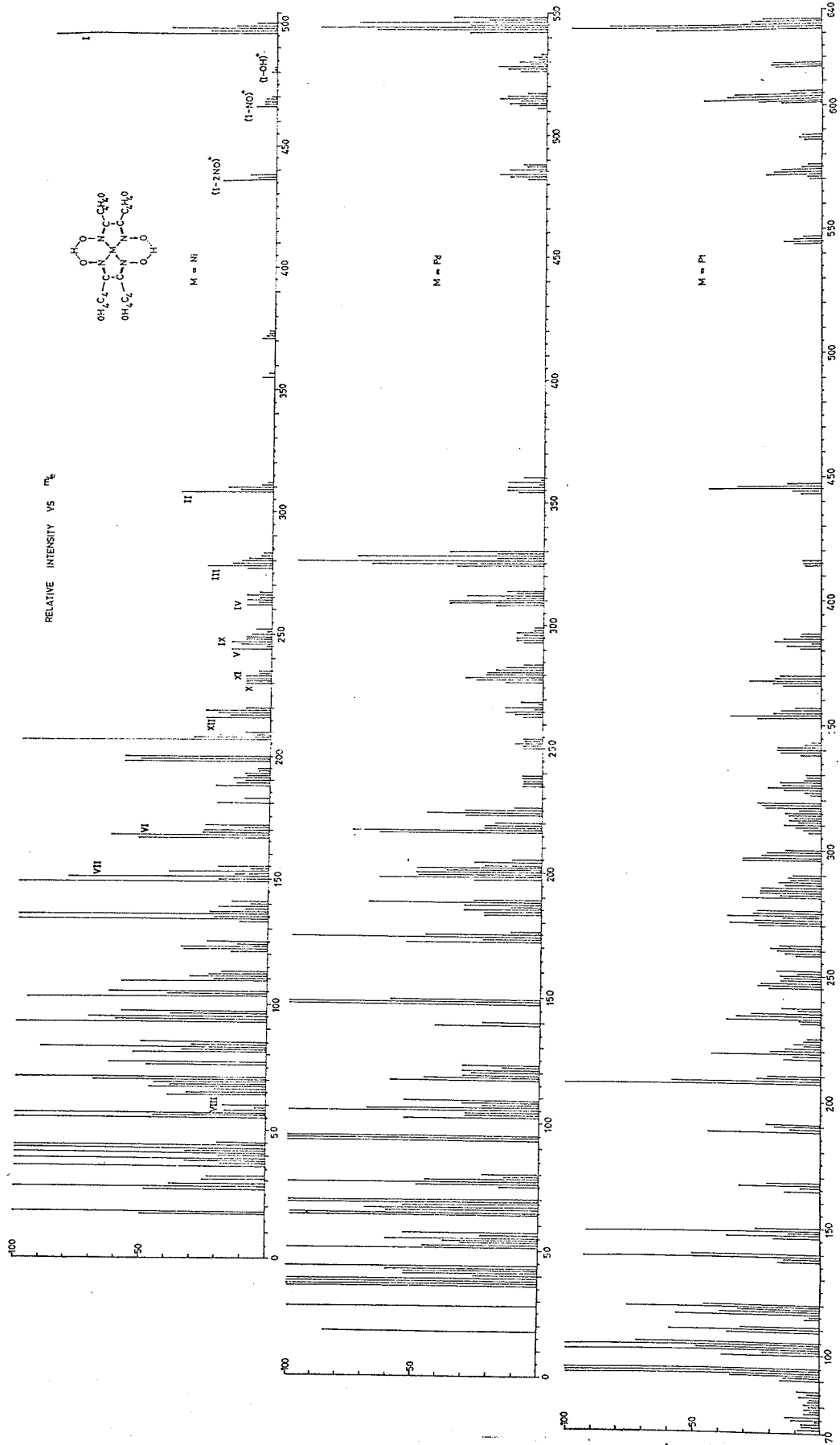
FIGS. 25 - 29

MASS SPECTRA OF VIC - DIOXIMATES

1. Dimethylglyoximates, page 67
2. Diphenylglyoximates, page 68
3.  $\alpha$ -Furildioximates, page 69
4. Nioximates, page 70
5. 4-methyl-nioximates, page 71









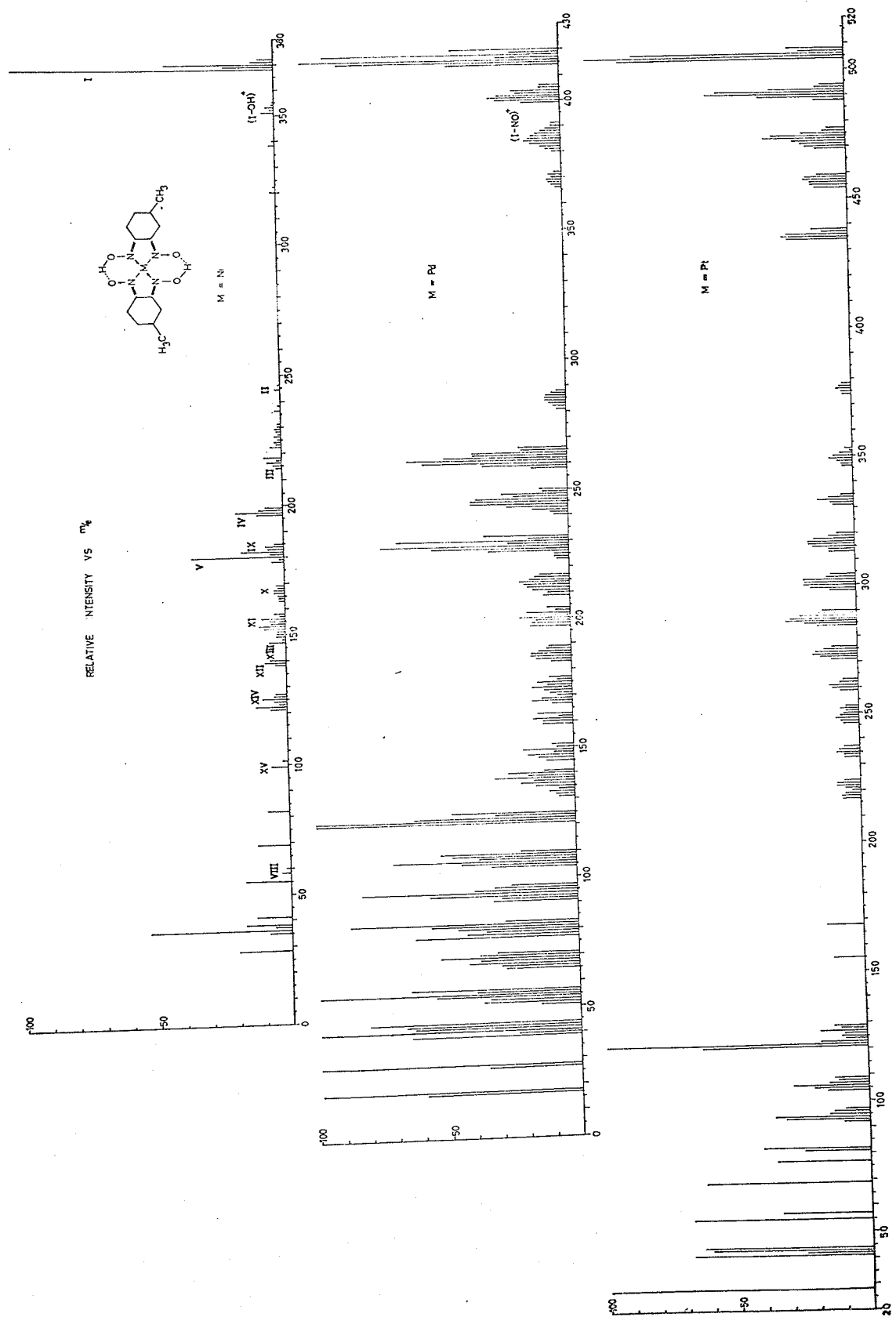
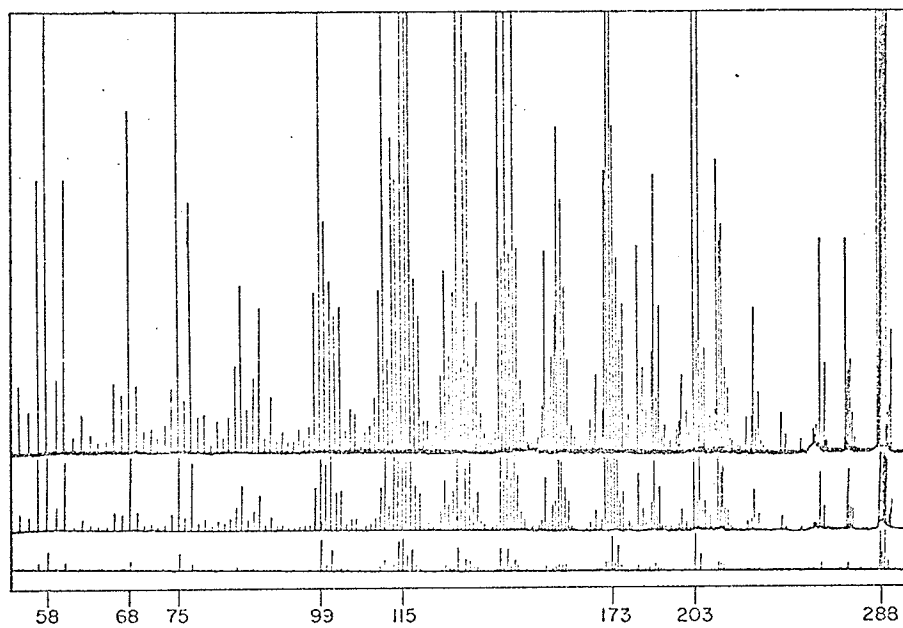
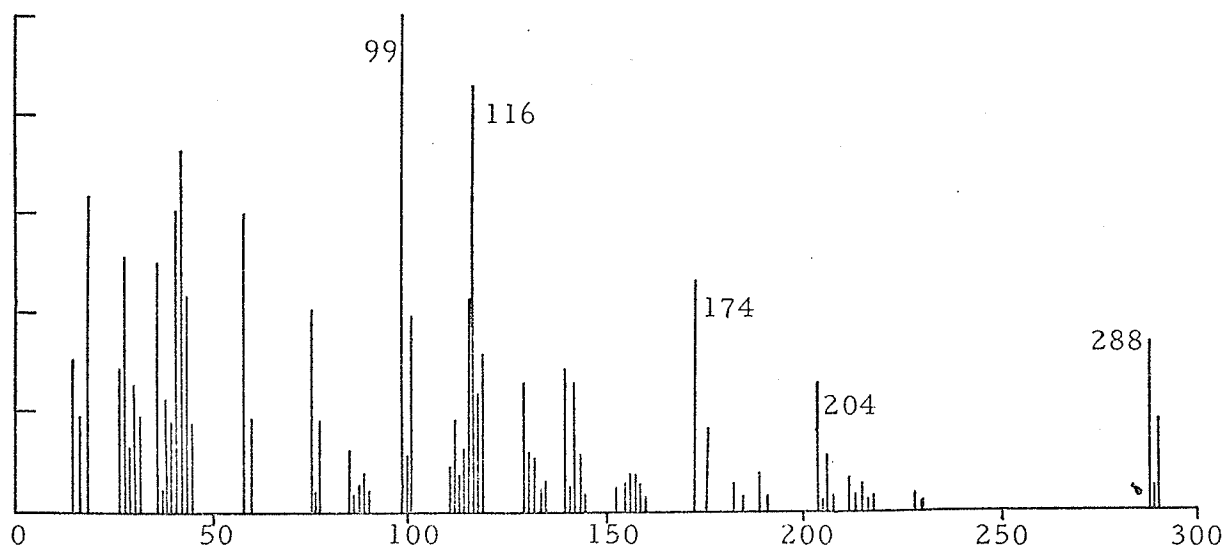


FIG. 30

COMPARISON OF MASS  
SPECTRA OF  $\text{Ni}(\text{DMG})_2$



(a) Jenkin and Majer's result



(b) Obtained in this work

TABLE VIII. SAMPLE TEMPERATURE, MASS/CHARGE RATIOS FOR METASTABLE AND DOUBLY-CHARGED ION PEAKS FOR DIMETHYLGLYOXIMATES

	Ni	Pd	Pt	Assignment
Temp. °C	200	185	170	
Metastable	-	-	-	
D. Charged Ion Peaks	144.5*	167.5(2)	212.5(27)	I <sup>++</sup>
	145.5	168.5	213.5	
	146.5		214.5	
	-	-	189.5	
			190.5	(I-47) <sup>++</sup>
			191.5	
			192.5	
	114.5	-	181.5(3)	(I-60) <sup>++</sup>
	115.5		182.5	
	94.5 - 96.5	-	165.5 - 168.5	(I-99) <sup>++</sup>
	-	-	108.5 - 109.5	
	73.5(2)	73.5-74.5(2)	-	
	59.5	-	-	
			50.5 - 52.5	

\* For this table and all subsequent tables, doubly-charged ions which have integral mass units are not listed

() Indicates measurable intensity of values quoted

TABLE IX. SAMPLE TEMPERATURE, MASS/CHARGE RATIOS FOR METASTABLE AND DOUBLY - CHARGED ION PEAKS FOR DIPHENYLGLYOXIMATES

	Ni	Pd	Pt	Assignment
Temp. °C	205	195	265	
Metastable	-	33.8 56.5	33.8 56.5	57 <sup>+</sup> - 44 <sup>+</sup> 105 <sup>+</sup> - 77 <sup>+</sup>
D. Charged Ion Peaks	269.5	291.5-293.5	336.5-337.5(15)	I <sup>++</sup>
	-	187.5-189.5	-	(I-208) <sup>++</sup>
	-	176.5	-	
	155.5-159.5	-	-	
	-	101.5-102.5	101.5-102.5	
	-	95.5-96.5	-	
	-	-	91.5-92.5	(N-C(C $\phi$ ) - $\phi$ ) <sup>++</sup>
	-	88.5	87.5-88.5	( $\phi$ - C $\equiv$ C - $\phi$ ) <sup>++</sup>
	-	-	58.5-59.5	
	-	45.5-49.5	45.5-49.5	
	-	37.5-38.5	37.5-38.5	C <sub>6</sub> H <sub>5</sub> <sup>++</sup>

TABLE X. SAMPLE TEMPERATURE, MASS/CHARGE RATIOS FOR METASTABLE AND DOUBLY-CHARGED ION PEAKS FOR  $\alpha$ -FURILDIOXIMATES

	Ni	Pd	Pt	Assignment
Temp. °C	85	110	280	
Metastable	-	-	-	
D. Charged Ion Peaks	248.5-249.5	270.5-271.5	316.5-317.5(5)	I <sup>++</sup>
	-	-	310.5-307.5	(I-30) <sup>++</sup>
	-	243.5-244.5	-	(I-60) <sup>++</sup>
	-	-	276.5-279.5	558 <sup>++</sup>
	-	225.5-227.5	-	
	-	-	214.5-215.5	
	-	-	188.5-189.5	V <sup>++</sup>
	115.5	-	177.5-179.5	X <sup>++</sup>
	-	-	162.5-163.5	(V-67) <sup>++</sup>
	108.5-109.5	108.5-109.5	108.5-109.5	
	96.5-99.5	96.5-99.5	98.5-99.5	
		82.5-88.5	87.5-88.5	
	63.5-66.5	-	61.5-63.5	
	57.5-59.5	58.5-59.5	-	
	(46.5-53.5)	(45.5-47.5)	45.5-47.5	
	37.5-38.5	-	34.5-36.5	

TABLE XI. SAMPLE TEMPERATURE, MASS/CHARGE RATIOS FOR METASTABLE AND DOUBLY - CHARGED ION PEAKS FOR NIOXIMATES

	Ni	Pd	Pt	Assignment
Temp. °C	130	105	120	
Metastable	306.9	354.7 59.5	443.4	$(P^+ \rightarrow (P-OH)^+)$ $108^+ \rightarrow 80^+$
D. Charged Ion Peaks	170.5-171.5	193.5-194.5	237.5-239.5(7)	$I^{++}$
	-	-	224.5(6)	$(I-30)^{++}$
	-	175.5-177.5	-	$(I-2OH)^{++}$
	-	-	203.5	$(I-72)^{++}$
	-	166.5-167.5	-	
	126.5-127.5	129.5-131.5	-	
	126.5-127.5	-	144.5-145.5	$X^{++}$
	10108.5	-	-	
	96.5-97.5	96.5-98.5	95.5-98.5	
	-	75.5-78.5	73.5-76.5	
	53.5-54.5	53.5-54.5	53.5-59.5	
	44.5-46.5	43.5-44.5	43.5-45.5	
	-	38.5-40.5	37.5-39.5	

TABLE XII. SAMPLE TEMPERATURE, MASS/CHARGE RATIOS FOR METASTABLE AND DOUBLY - CHARGED ION PEAKS FOR 4 - METHYL - NIOXIMATES

Temp. °C	Ni	Pd	Pt	Assignment
Metastable	334.8	382.7 37.5	471.5	$P^+ \rightarrow (P - OH)^+$
D. Charged Ion Peaks	183.5-184.5	207.5-209.5(2)	252.5-253.5(9)	$I^{++}$
	175.5-177.5	-	242.5-244.5	$(I - OH)^{++}, (I - CH_3)^{++}$
	-	-	225.5-229.5(5)	$(I - 48)^{++}$
	-	132.5-133.5	172.5-178.5	$III^{++}$
	166.5-167.5	166.5-167.5	-	
	118.5-120.5	-	-	
	71.5	98.5-101.5	141.5-144.5	$XII^{++}$
	-	84.5-87.5	137.5-138.5	$XIII^{++}$
	71.5-74.5	72.5-73.5	73.5-74.5	
	-	-	119.5-120.5	
	-	-	114.5-117.5	
	-	-	105.5-108.5	
	-	98.5-101.5	98.5-101.5(9)	
	59.5-61.5	59.5-61.5	59.5-61.5	
	-	45.5-47.5	45.5-47.5	

metal-dioximates has roughly the same volatility under operating conditions of the mass spectrometer. These temperatures, however, should not be taken to be too accurate a measurement of their ease of sublimation; but they do indicate that under specified operation conditions, nickel and palladium  $\alpha$ -furildioximates have the highest and diphenyglyoximates the lowest volatility.

For ease in making comparisons between the spectra of chelates of the same ligand with the three metals; the spectra are reproduced in the same figure (Figs. 25 - 29) so that metal-containing ions formed by loss of neutral species of the same mass fall vertically above or below each other. Metal-containing ions are readily recognized by their isotopic patterns. This method of presentation permits equivalent ions to be readily recognized. Ions which do not contain a metal atom are also easily compared since ions of the same composition appear at the same values of  $m/e$ . For ions which contain Pd or Pt, and which differ by one or more hydrogen atoms, a complex pattern of peaks resulted, which in some cases was not readily resolved.

The mass spectra of organic compounds have been rationalized in terms of the preferred tendency towards formation of even-electron ions. For compounds which contain transition metal atom, a similar rationalization has been made in which it is assumed that the rest of the ion can become even electron by transfer of an unpaired electron to the d orbitals of the metal

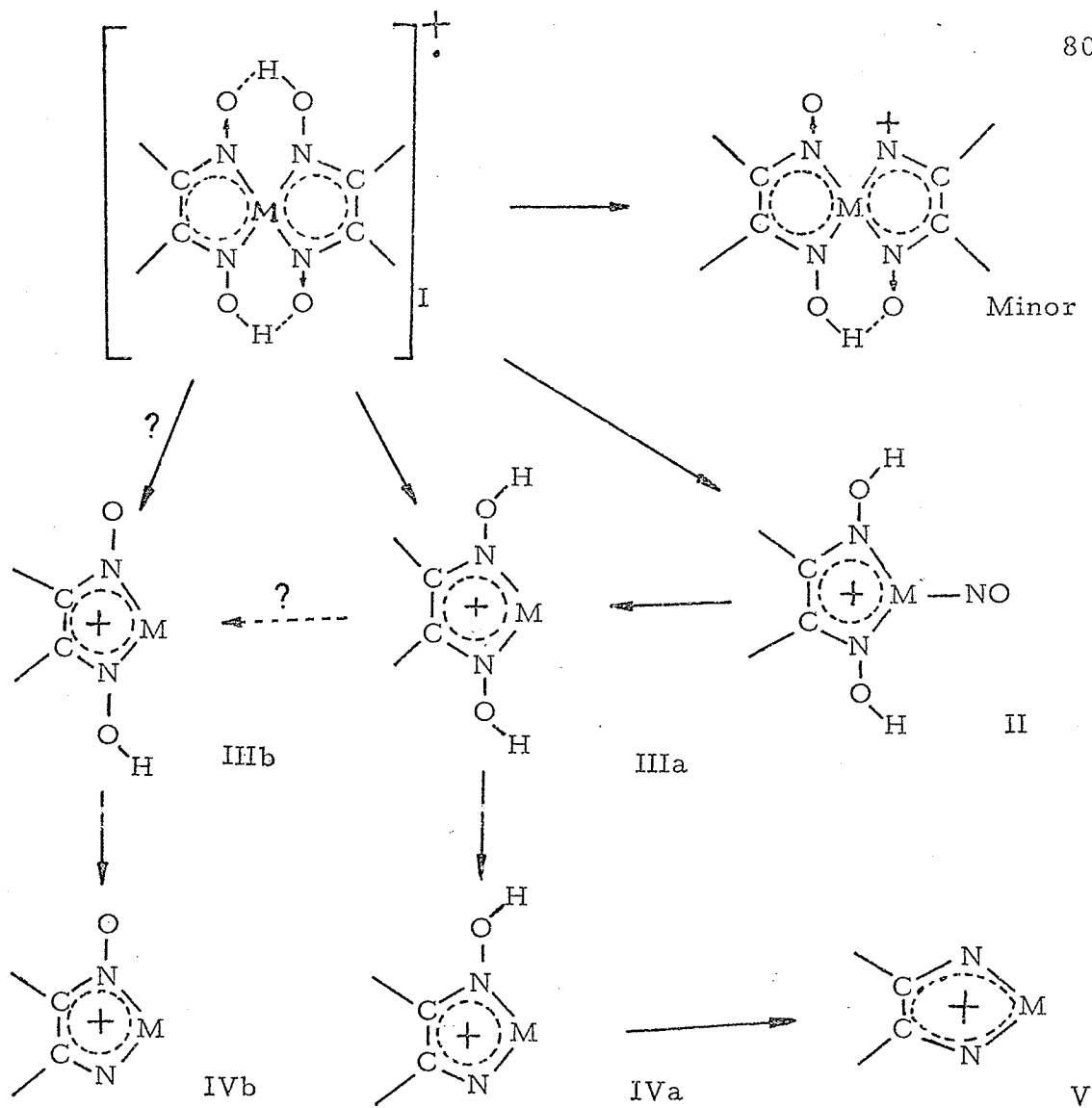
atom, resulting in a formal change in the valency state of the metal atom. (52, 61)

In fig. 31 is shown a tentative fragmentation scheme showing the more important ionic decompositions. This scheme should be regarded as speculative since the absence of meta-stable peaks in the spectra, except in some cases for the transition  $P^+ \rightarrow (P - OH)^+$ , means that there is no confirmation for any given transition (page 63). Attempts have been made to rationalize trends in the mass spectra of transition metal  $\beta$ -diketonates, but trends between the various vic-dioxime complexes are more difficult to find.

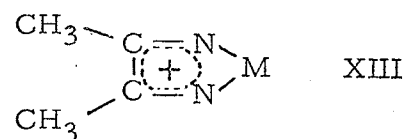
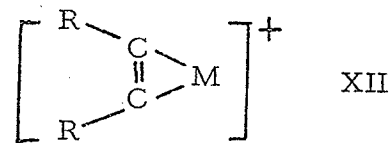
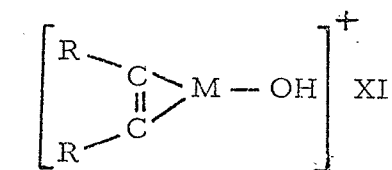
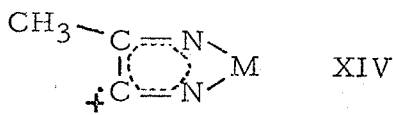
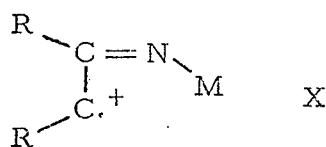
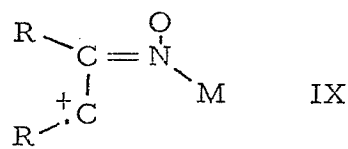
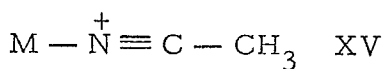
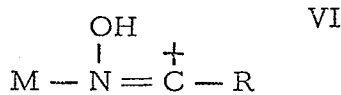
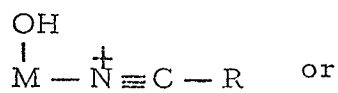
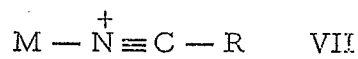
Removal of an electron from the neutral chelate results in an ion which has been formulated as I, in which the positive charge may be delocalized over one or two chelate rings. Such a conclusion is based on the following assumption. In the solid state, the neutral complex  $Ni(DMG)_2$  is perhaps best represented as shown in table I, page 2, since the ring C — C bond, after complexation, lengthens its bond length to that of a single bond and thus there is no interaction between the oxime groups. (10) The short metal-nitrogen bonds can only be ascribed to increased  $\sigma$ -bond strength relative to an octahedral complex and not as a result of delocalization of the  $\pi$ -electrons. For, if the out of plane  $\pi$ -bonding is of any importance, electron delocalization over the whole ring should occur, by analogy with thiophene in which sulfur uses the  $d_{xz}$ ,  $d_{yz}$  and  $p_z$  orbitals (77), furan, and pyrrole in which oxygen and nitrogen use the s and p

FIG. 31

SCHEMATIC DIAGRAM OF FRAGMENTATION  
PATTERN OF VIC-DIOXIMATES



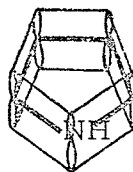
Other fragment ions:



hybridized orbitals, and the ring C — C bond should be shorter than a normal single bond. For square planar complexes, multiple



Thiophene

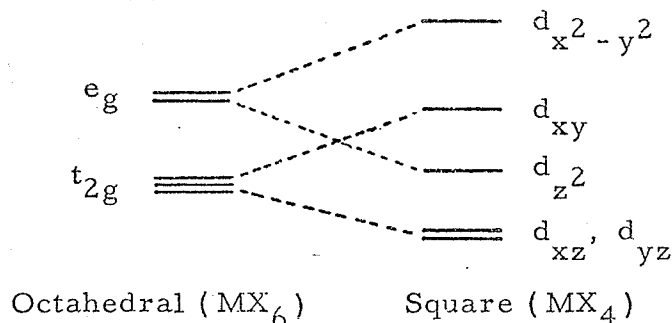


Pyrrole

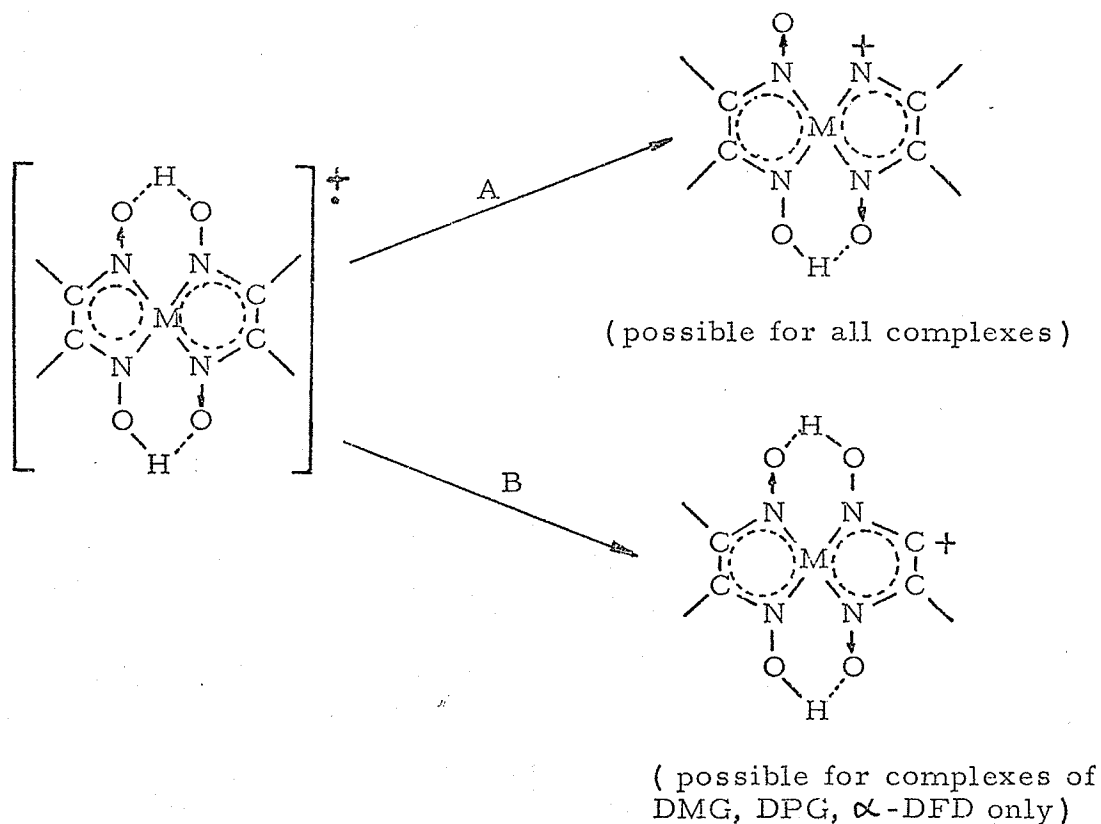
bonding between metal and ligand can occur with the metal using  $d_{xz}$ ,  $d_{yz}$  and  $p_z$  orbitals. Multiple bonding between metal and ligand results in a reduction of negative charge on the metal-atom and requires the availability of low energy acceptor orbitals on the ligand. For these vic-dioxime ligands, the available acceptor orbitals of lowest energy are the  $\pi^*$  orbitals. However, in a molecular orbital treatment of square planar complexes in which  $\pi$ -bonding is possible, Gray and Ballhausen (78) suggest that in  $\pi$ -bonding between metal and ligand the metal  $p_z$  orbital and the ligand  $\pi$  orbitals make the major contribution. The addition of a fifth ligand above the square plane decreases the  $\pi$ -bonding by tying up the  $p_z$  orbital in  $\sigma$ -bonding. In the solid  $\text{Ni}(\text{DMG})_2$  complex, metal-metal bonds have been proposed ( Yamada and Tsuchida, Banks and Caton, Banks and Barnum, Godycki and Rundle, page 5), and in fact is said to have been detected through semiconductivity considerations ( Thomas and Underhill, page 6), to explain solubility and other properties such as abnormal dichroism of the complex (page 5) although there is still disagreement on this point (Ingraham,

Anex and Krist, page 5). This bonding has invoked the use of  $d_z^2 p_z$  hybrid orbitals and may account for the apparent lack of  $\pi$ -bonding between metal and ligand in the solid state. In the vapour state, discrete molecules of the chelate exist, and the  $p_z$  orbital becomes available for  $\pi$ -bonding. Such  $\pi$ -bonding is probably of importance in explaining the stabilities of the chelates under electron impact since it provides a mechanism by which a positive charge can become delocalized. The existence of doubly-charged ions (tables VIII - XII) which is characteristic of a conjugated system, particularly fused rings, seems to support the above proposition.

The low relative abundances of the  $(P - OH)^+$  peaks for all chelates, and of  $(P - CH_3)^+$ ,  $(P - C_6H_5)^+$  and  $(P - C_4H_4O)^+$  peaks for the  $M(DMG)_2$ ,  $M(DPG)_2$  and  $M(\alpha\text{-DFD})_2$  chelates respectively, suggests that upon ionization of the chelate molecule, an electron is either removed from a metal-dominated orbital, or that if an electron is removed from a ligand-dominated orbital, considerable stabilization of the chelate ring by the metal ion occurs. Koopmans' theorem (79) would predict that upon ionization, an electron would be removed from a metal-dominated orbital, since ligand field theory places one of these ( $d_{xy}$ ) as the occupied



orbital of highest energy in the neutral complexes. Electron impact studies with  $\beta$ -diketonate complexes suggest that Koopman's theorem may not be valid for all transition metal complexes, however, and the possibility of removal of a ligand electron cannot be excluded. If a ligand electron is removed then unless stabilization of the chelate ring by the metal atom occurs, the ready loss of  $\cdot\text{OH}$  (or  $\cdot\text{CH}_3$ ,  $\cdot\text{C}_6\text{H}_5$  or  $\cdot\text{C}_4\text{H}_4\text{O}$  for the  $\text{M}(\text{DMG})_2$ ,  $\text{M}(\text{DPG})_2$  and  $\text{M}(\alpha\text{-DFD})_2$  complexes respectively) would be expected, since in this way, a stable even-electron ion would result by transfer of one electron of the ring-to-substituent bond to the C—N bond, as in reactions A or B:



The  $(P - CH_3)^+$  peak is observed for the 4-methyl-nioxime complexes but in these chelates, the methyl radical is lost from the cyclohexane ring. The low intensity of the  $(P - OH)^+$  and  $(P - R)^+$  peaks thus suggests that the metal can stabilize the molecular ion by multiple bonding to the ligand.

In both cases, formation of the doubly-charged ions can be accounted for. Two electrons can either be removed from the metal-dominated ( $d_{xy}$ ) orbital or from the  $\pi$ -systems of the  $C = N$  bonds.

Whether, or not, the initial ionization process is caused by removal of an electron from a metal-dominated or ligand-dominated orbital is not important since the process is very fast compared with the atomic motions and the molecular ion has time to reach equilibrium in its electronic states before fragmentation occurs (page 56). Consequently stabilization of the molecular ion could occur via multiple bonding between the metal and the ligand.

The intensity of the  $(P - OH)^+$  ion increases in the sequence  $Ni < Pd < Pt$  in each series of the dioximates. This is the opposite of the trend expected since  $p_z$  orbital participation in  $\pi$ -bond formation might be expected to increase as the size of the  $p_z$  orbital increases ( $4p_z$ ,  $5p_z$  and  $6p_z$  for nickel, palladium and platinum respectively). This in turn would increase the strength of the  $N - OH$  bonds in the order  $Ni < Pd < Pt$  and so the intensities of the  $(P - OH)^+$  ions should be in the reverse order. On the other

hand, the ionization potential increases in the sequence  $\text{Ni} < \text{Pd} < \text{Pt}$  ( $7.6 < 8.3 < 8.8$  eV), making electron release to the ligand more difficult. Stabilization ability can also be offset by atomic sizes of these respective metal atoms so that  $\text{Pt(II)}$  complexes are under more strain and thus less stable (77) with respect to the  $\text{Ni(II)}$  complexes ( $\text{Ni(DMG)}_2$  has  $\text{N}-\text{C}-\text{C}$  bond angles of  $109^\circ$  and  $113^\circ$  while  $\text{Pt(DMG)}_2$  has  $\text{N}-\text{C}-\text{C}$  bond angles of  $113^\circ$  and  $117^\circ$ , table II, page 3). The decrease in intensity of the  $(\text{P}-\text{OH})^+$  from  $\text{Pt(II)}$  to  $\text{Ni(II)}$  complexes might occur if the  $4p_z$  and  $5p_z$  orbitals of Pd and Pt respectively, though more extended, are less effective than the nickel  $3p_z$  orbital in interacting with the  $2p$  orbitals of the ligand  $\pi$  system. In addition, any subsequent fragmentation of the  $(\text{P}-\text{OH})^+$  would also depend upon the nature of the metal, so that, at present the trend in the relative intensities of these ions is regarded as a phenomenological one.

A preferred decomposition of the molecular ion results in the even-electron ion formulated as II, by the loss of  $\text{NOCCH}_3\text{CCH}_3$ , likely as  $\text{NO} + \text{CH}_3\text{C}\equiv\text{CCH}_3$ , although this cannot be confirmed. (It is possible in this decomposition that a metal-hydrogen bond is formed but there is little evidence in the rest of the spectra to support this possibility).

Other abundant ions in the spectra are those formulated as IIIa or IIIb. Isotopic ratio and intensity calculations show that both species are present, with a more abundant than b in all cases

III and IV (Table XIII). The precursor of IIIb is likely I but of IIIa could be I or II, or both. IVa and IVb may be formed by loss of  $\cdot\text{OH}$  from IIIa and IIIb respectively. The ion V may be formed from IVa by loss of an  $\cdot\text{OH}$  radical but other fragmentations lead to ions in which the ring structure of the chelate is not possible. Furthermore, for the nioxime and 4-methyl-nioxime complexes, ions now appear in which fragmentation of the cyclohexane ring occurs. It does not seem worthwhile to extend the fragmentation scheme to include these ions, since it would be highly speculative and the intermediate precursors of the ions are not known. It suffices to say that common ions can be recognized in both the nioxime and 4-methyl-nioxime complexes and a few of these can also be found in the dimethylglyoxime complexes (for example ions XIII, XIV and XV in the spectra of nioximates and 4-methyl-nioximates).

Possible structures of some other more abundant ions are given at the bottom of the fragmentation scheme and little comment will be given because, as mentioned earlier, the fragmentation paths and precursor ions are unidentified. Two points might be noted:

(1) The migration of a  $\cdot\text{OH}$  radical to the metal atom can be confirmed as ions can be identified in which a  $\text{M}-\text{OH}$  bond must be present (for example, ions XI (and VI)). A peak of  $m/e = 75$  (which is the  $\text{NiOH}^+$  ion) in the nickel dimethylglyoxime complex is very intense and its analogs in the palladium and platinum complexes are absent.

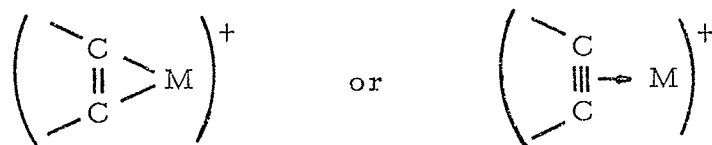
Species Metal	II <sup>+</sup>	(II-H) <sup>+</sup>	IIIa	IIIb	IIIc	IVa	IVb
Ni	m/e 204 87 (100)	203 13	174 83 (69)	173 15 (24)	172 2 (7)	157 62	156 38
Pd	m/e 252 100	251 0	222 51	221 49	220 0	205 65	204 35
Pt	m/e 341 -	340 -	311 33	310 19	309 48	294 50	293 50

TABLE XIII. ISOTOPIC RATIO AND INTENSITY CALCULATIONS  
OF SOME SPECIES OF DIMETHYLGLYOXIMATES

Values in brackets are those obtained from the deuteriated compound

This indicates the stronger tendency for nickel to form a divalent compound (in agreement with their accepted chemistry). It is interesting to note that only the nickel dimethylglyoximate and not the other nickel complexes gives this peak and at such high intensity (40%).

(2) The three metals are known to form stable  $\pi$ -allyl complexes, especially platinum. The spectra show the presence of the species



with intensities 15, 13 and 23 for the Ni, Pd and Pt dimethylglyoximates. This is what would be expected if the relative intensities of the ion peaks are a measure of their relative stability.

CHAPTER FOUR  
SUMMARY AND CONCLUSIONS

From thermogravimetric analysis, it is shown that all vic-dioxime complexes of Ni(II), Pd(II) and Pt(II) are stable up to at least 250°C. Decomposition reactions are exothermic and oxygen catalyzes or at least takes part in the decomposition reactions. From the decomposition temperature values, it is found that the platinum complexes are in general thermally less stable than the palladium and nickel complexes, contrary to other square planar complexes of the same group of metals. That they do not decompose below 250°C makes explanation of the mass spectra feasible.

The mass spectra of these vic-dioximates are complex and they suggest participation of the metal  $p_z$  orbital in stabilizing the various ionic species through delocalization of the positive charge. The trends between the various metals and ligands are not clearly defined, although the palladium species may give a higher abundance of non-metal-containing ions. Participation of the metal  $p_z$  orbital in the stabilization of the ions might be expected to increase as the ease of oxidation of the metal increases, i. e.  $Ni < Pd \approx Pt$ . This effect is not readily apparent and it may be that the  $4p_z$  and  $5p_z$  orbitals of Pd and Pt respectively, though more extended, are less effective than the Ni  $3p_z$  orbital for electron delocalization through the  $\pi$ -bond formed as a result of the interaction between this  $p_z$  orbital and the  $\pi$ -system of the ligand. However, it has proved extremely difficult to predict and rationalize trends in these spectra with the information available at present.

## BIBLIOGRAPHY

1. Vic-dioximes are those which have the oxime group on adjacent carbon atoms.
2. E. Frasson, C. Panattoni and R. Zannetti, *Acta Cryst.* 12, 1207 (1959).
3. E. O. Schlemper, *Inorg. Chem.* 7, 1130 (1968).
4. E. Frasson and C. Panattoni, *Acta Cryst.* 13, 893 (1960).
5. E. Frasson, R. Bardi and S. Bezzi, 12, 201 (1957).
6. L. Edward Godycki, R. E. Rundle, R. C. Voter and C. V. Banks, *J. C. P.* 19, 1205 (1951).
7. L. E. Godycki and R. E. Rundle, *Acta Cryst.* 6, 487 (1953).
8. D. E. Williams, G. Wohlaer and R. E. Rundle, *J. A. C. S.* 81, 755 (1959).
9. R. Blinc and D. Hadzi. *J. C. S.*, 4536 (1958).
10. B. G. Anex and F. Kevin Krist, *J. A. C. S.* 89, 6114 (1967).
11. B. Basu, G. M. Cook and R. L. Belford, *Inorg. Chem.* 3, 1361 (1964).
12. S. Thompson and A. G. Malton, Nucleation of Dimethylglyoximes, U. S. A. E. C., 1967. (COO-582-14).
13. L. Gordon, O. E. Hileman Jr. and P. R. Ellefsen, *Pure and Appl. Chem.* 13, 497 (1966).
14. J. C. Zahner and H. G. Drickamer, *J. C. P.* 33, 1625 (1960).
15. F. P. Dwyer and D. P. Mellor, Chelating Agents and Metallic Chelates, p. 10, Academic Press, 1964.
16. A. G. Sharpe and D. B. Wakefield, *J. C. S.* 281, (1957).
17. S. C. Ogburn Jr. *J. A. C. S.* 48, 2493, (1926).
18. R. G. Voter, C. V. Banks and H. Diehl, *Anal. Chem.* 458 (1948), 652 (1948).

19. R. Blinc and D. Hadzi, *Spect. Acta*, 16, 852 (1960).
20. S. Yamada and R. Tsuchida, *Bull. Chem. Soc. Japan*, 27, 156 (1953).
21. J. E. Caton and C. V. Banks, *Talanta* 13, 967 (1966).
22. C. V. Banks and D. W. Barnum, *J. A. C. S.* 80, 4767 (1958).
23. R. E. Rundle and C. V. Banks, *J. P. C.* 67, 508 (1963).
24. L. L. Ingraham, *Acta Chemica Scandinavica* 20, 283 (1966).
25. T. W. Thomas and A. E. Underhill, *Chem. Comm.* 725 (1969).
26. S. N. Bhat, G. V. Chandrashekar and C. N. Rao, *Inorg. Nucl. Chem. Letters*, 3, 409 (1967).
27. W. Huckel, *Structural Chemistry of Inorganic Compounds*, p. 144, Elsevier Publishing Company (1950).
28. W. Wendlandt and J. P. Smith, *The Thermal Properties of Transition-metal Amine Complexes*, p. 13, Elsevier Publishing Company (1967).
29. K. Honda, *Scien. Reports, Tohoku Imp. Univ.*, 4, 97 (1915).
30. E. L. Simons and A. E. Newkirk, *Talanta* 11, 549 (1964).
31. A. E. Newkirk, *Anal. Chem.* 32, 1558 (1960).
32. C. Duval, *Inorganic Thermogravimetric Analysis*, Elsevier Publishing Company (1963).
33. W. Wendlandt, W. Robinson and W. Y. Tang, *Inorg. Nucl. Chem.* 25, 1495 (1963) and references therein.
34. Accompanied Cahn RG - Electrobalance Manual.
35. P. D. Garn, *Anal. Chem.* 29, 839 (1957).
36. C. Duval, *Inorganic Thermogravimetric Analysis*, p. 163, Elsevier Publishing Company (1963).

37. J. Zsako, C. Várhelyi and E. Kékedy, *Inorg. Nucl. Chem.* 28, 2637 (1966).
38. H. Horowitz and G. Metzger, *Analyst. Chem.* 35, 1464 (1963).
39. C. Duval, *Inorganic Thermogravimetric Analysis*, p. 367, 475 and 591, Elsevier Publishing Company (1963).
40. G. A. Errock, *Mass Spectrometry*, p. 1, Academic Press (1965).
41. J. J. Thomson, *Rays of Positive Electricity*, Longmans, London (1913).
42. F. W. Aston, *Mass Spectra and Isotopes*, Arnold, London (1942).
43. A. J. Dempster, *Phys. Rev.* 11, 316 (1918).
44. A. E. Cameron and D. F. Eggers, *Rev. Sci. Instr.* 19, 605 (1948).
45. R. D. Craig et. al., *Chimica* 17, (1963).
46. A. O. Nier, *Sci. Inst.* 11, 212 (1940).
47. J. Mattauich and R. Herzog, *Z. Physik* 89, 786 (1934).
48. H. M. Rosenstock, M. B. Wallenstein, A. L. Wahrhaftig and H. Eyring, *Proc. Natl. Acad. Sci.* 38, 667 (1952).
49. W. A. Chupka, *J. C. P.* 30, 191 (1959).
50. M. Vestal, A. L. Wahrhaftig and W. H. Johnston, *J. C. P.* 37, 1276 (1962).
51. J. W. Warren, *Nature* 165, 810 (1950).
52. C. G. MacDonald and J. S. Shannon, *Aust. J. Chem.* 19, 1545 (1966).
53. R. Jayaram, *Mass Spectrometry*, Plenum Press, N. Y. (1966).
54. C. Reichert, J. B. Westmore and H. G. Gesser, *Chem. Comm.* 782 (1967) and references therein.
55. E. P. Dudek, E. Chaffee and G. Dudek, *Inorg. Chem.* 7,

- 1257 (1968).
56. C. Reichert, Daniel K. C. Fung, Denis C. K. Lin and J. B. Westmore, *Chem. Comm.* 1094 (1968).
  57. F. Lewis and B. F. G. Johnson, *Accounts Chem. Res.*, 1, 245 (1968).
  58. R. W. Kiser and R. E. Sullivan, *Anal. Chem.* 40, 273R (1968).
  59. F. Jonhson, *J. Organometallic Chem.* 3, 233 (1965).
  60. M. Bancroft; C. Reichert, J. B. Westmore and H. D. Gesser, *Inorg. Chem.* 8, 474 (1969).
  61. A. E. Jenkins and J. R. Majer, *Talanta* 14, 777 (1967).
  62. A. G. Sharkey, Jr., C. F. Robinson and R. A. Friedel, *Advances in Mass Spectrometry*, p. 195, Pergamon Press, (1959).
  63. J. Franck, *Trans. Faraday Soc.* 21, 536 (1926)
  64. E. U. Condon, *Phys. Rev.* 32, 858 (1928).
  65. R. W. Kiser, *Introduction to Mass Spectrometry and Its Application*, p. 121, Prentice Hall Inc. (1965).
  66. H. C. Hill, *Introduction to Mass Spectrometry*, Hyden and Son Ltd. (1966).
  67. C. A. McDowell, *Mass Spectrometry*, McGraw Hill Book Company Inc. (1963).
  68. J. A. Hipple, R. E. Fox and E. U. Condon, *Phys. Rev.* 69, 347 (1946).
  69. N. D. Coggeshall, *J. C. P.* 37, 2167 (1962).
  70. J. Momigny, *Bull. Soc. Chim. Belge.* 70, 291 (1961).
  71. J. Hartel and Ch. Ottinger, *Z. Naturf.* 22a, 40 (1967).
  72. H. M. Rosenstock, *Advances in Mass Spectrometry*, Vol. 4, p. 523, Elsevier Publishing Company, N. Y. (1968).  
H. M. Rosenstock and M. Krauss, *Advances in Mass*

Spectrometry, Vol. 2, p. 256, Pergamon Press Book,  
McMillan Company, N. Y. (1963).

73. G. R. Lester, Mass Spectrometry, p. 170, Academic Press,  
(1963).
74. J. H. Beynon, Mass Spectrometry and Its Application to  
Organic Chemistry, p. 282, 344, 401, Elsevier Company,  
N. Y. (1960).
75. M. Solomon and A. Mandelbaum, Chem. Comm. 890 (1969).
76. L. E. Godycki, R. E. Rundle, R. C. Voter and C. V. Banks,  
J. C. P. 19, 1205 (1951), 37, 2167 (1962).
77. L. S. Bark and D. Brandon, Talanta 14, 759 (1967).
78. H. B. Gray, C. J. Ballhausen, J. A. C. S. 85, 260 (1963).
79. T. Koopmans, Physica 1, 104 (1933).